Atmospheric
Chemistry
and Physics

Open Access

The balances of mixing ratios and segregation intensity: a case study from the field (ECHO 2003)

R. Dlugi[1], M. Berger[1], M. Zelger[1], A. Hofzumahaus[2], F. Rohrer[2], F. Holland[2], K. Lu[2,*], and G. Kramm[3]

[1]Arbeitsgruppe Atmosphärische Prozesse (AGAP), Munich, Germany
[2]Institut für Energie- und Klimaforschung: Troposphäre, Forschungszentrum Jülich, Germany
[3]University of Alaska, Fairbanks, AK, USA
[*]now at: Peking University, College of Environmental Sciences and Engineering, Beijing, China

Correspondence to: R. Dlugi (rdlugi@gmx.de) and A. Hofzumahaus (a.hofzumahaus@fz-juelich.de)

Abstract. An inhomogeneous mixing of reactants causes a reduction of their chemical removal compared to the homogeneously mixed case in turbulent atmospheric flows. This can be described by the intensity of segregation I_S being the covariance of the mixing ratios of two species divided by the product of their means. Both terms appear in the balance equation of the mixing ratio and are discussed for the reaction between isoprene and OH for data of the field study ECHO 2003 above a deciduous forest. For most of these data, I_S is negatively correlated with the fraction of mean OH mixing ratio reacting with isoprene. I_S is also negatively correlated with the isoprene standard deviation. Both findings agree with model results discussed by Patton et al. (2001) and others. The correlation coefficient between OH and isoprene and, therefore, I_S increases with increasing mean reaction rate. In addition, the balance equation of the covariance between isoprene and OH is applied as the theoretical framework for the analysis of the same field data. The storage term is small, and, therefore, a diagnostic equation for this covariance can be derived. The chemical reaction term R_{ij} is dominated by the variance of isoprene times the quotient of mixing ratios of OH and isoprene. Based on these findings a new diagnostic equation for I_S is formulated. Comparing different terms of this equation, I_S and R_{ij} show a relation also to the normalised isoprene standard deviation. It is shown that not only chemistry but also turbulent and convective mixing and advection – considered in a residual term – influence I_S. Despite this finding, a detection of the influence of coherent eddy transport above the forest according to Katul et al. (1997) on I_S fails, but a relation to the turbulent

and advective transport of isoprene variance is determined. The largest values of I_S are found for most unstable conditions with increasing buoyant production, confirming qualitatively model predictions by Ouwersloot et al. (2011).

1 Introduction

Mixing and simultaneous chemical reactions of trace gases in the atmospheric boundary layer (ABL) are shown to be influenced by the turbulent regimes of the fluid and convection as well as the oxidation potential of the atmosphere (e.g. Seinfeld and Pandis, 1997; Finlayson-Pitts and Pitts Jr., 1986; Lamb and Seinfeld, 1973; Donaldson, 1975). The early formulations of spatially resolved models to predict the development of photochemical air pollution considered therefore chemical reactions – mainly of first, second and third order – in a way that not only mean mixing ratios $\overline{c_i}$ and their products (e.g. $\overline{c_i} \times \overline{c_j}$ for a second-order reaction) together with the rate constant k_{ij} appear in the rate equations, as determined from laboratory experiments (e.g. Finlayson-Pitts and Pitts Jr., 1986), but also additional terms like variances and covariances $\overline{c_i' c_j'}$ have to be considered (e.g. O'Brien, 1971; Lamb and Seinfeld, 1973; Shu, 1976; McRae et al., 1982; Donaldson and Hilst, 1972; Donaldson, 1975; Lamb and Shu, 1978). Here c_i' and c_j' denote temporal fluctuations around the mean mixing ratios $\overline{c_i}$ and $\overline{c_j}$ of compounds i and j, respectively. If for a second-order reaction the product of the mean mixing ratios fulfills the relation $\overline{c_i} \times \overline{c_j} \gg \overline{c_i' c_j'}$, the influence of turbulent fluctuating terms in the reaction

rate equation $k_{ij}(\overline{c_i} \times \overline{c_j} + \overline{c'_i c'_j})$ can be neglected for the prediction of either mean value $\overline{c_i}$ or $\overline{c_j}$ (e.g. Shu, 1976). The same conditions are valid if the balances of higher-order moments (e.g. variances and covariances) are considered (e.g. Donaldson, 1975; McRae et al., 1982). If this inequality is not valid, higher-order moments have to be determined. The quotient of the covariance term and the product of the means is often called the intensity of segregation I_S and is applied to describe the degree of inhomogeneous mixing. As a consequence of this Reynolds-type ensemble averaging of properties of a fluid, one concept to describe the influence of fluctuations on chemical reactions is to introduce additional differential equations to determine higher-order moments (e.g. Donaldson and Hilst, 1972; Donaldson, 1973, 1975; Shu, 1976). Another is to find the exact properties of the probability density functions of turbulent quantities for each reactant (e.g. O'Brien, 1971; Bencula and Seinfeld, 1976; Lamb and Shu, 1978).

The balance equation approach was applied for the analysis of field studies of the NO_2–NO–O_3 system (e.g. Lenschow, 1982; Vilà-Gureau de Arellano and Duynkerke, 1992; Vilà-Guerau de Arellano et al., 1993; Kramm and Meixner, 2000) as well as modelling of the same system but for more complex atmospheric mixtures (e.g. McRae et al., 1982; Verver et al., 2000; Krol et al., 2000; Ebel et al., 2007; van Stratum et al., 2012). In addition, also fundamental studies were performed with large eddy simulation (LES) models on the general behaviour of slow, fast and very fast reacting compounds in the ABL mainly under the influence of free convective mixing conditions (e.g. Schumann, 1989; Verver et al., 1997; Vinuesa and Vilà-Guerau de Arellano, 2005; Ouwersloot et al., 2011). Comparing their results, the inhomogeneously mixed reactants – especially in the case of bimolecular reactions – can have reaction rates significantly different from the well-mixed case.

It is suggested by different authors (e.g. Krol et al., 2000; Pugh et al., 2011; Ouwersloot et al., 2011) that also the spatially inhomogeneous distribution of emission sources directly influences the segregation intensity I_S.

Most of these studies applied the Damköhler number Da_c, the quotient (τ_t/τ_c) between the characteristic mixing timescales of turbulent or convective processes τ_t and the specific chemical reaction τ_c, for a classification of I_S as a function of nearly inert ($Da_c \ll 1$), slow ($0.05 \lesssim Da_c \lesssim 0.5$), fast ($0.5 \lesssim Da_c \lesssim 5$) and very fast ($Da_c > 5$) bimolecular reactions.

In addition, an extended scaling uses the turbulent flux of a species $(\overline{w'c'_i})$ to find a description for reaction and inhomogeneous mixing (e.g. Schumann, 1989; Verver et al., 2000) and adds a second Damköhler number Da_f for the specific flux to this ranking concept. It seems that for many trace substances turbulent mixing ($0.01 < Da_c < 50$) significantly influences volume mean reaction rates and, therefore, also the budgets of trace gases (e.g. Verver et al., 2000; Ebel et al., 2007; Stockwell, 1995).

One should be aware that, depending on the concentration scales and the concepts applied for the calculation of τ_t, the numerical Da_c values may differ from each other (e.g. Schumann, 1989; Sykes et al., 1994; Verver et al., 1997, 2000). But despite such differences the ranking of reactions being most influenced by inhomogeneous mixing is consistent within each scaling concept.

One of the chemical components studied beside the system NO_2–NO–O_3 is the biogenic compound isoprene and the reaction with OH. After emission isoprene is mixed by turbulence and convection while being transported by the wind field. This compound reacts with OH (e.g. Finlayson-Pitts and Pitts Jr., 1986) which itself, as a fast reacting compound with $\tau_c < 1$ s, has only local sources and sinks. Therefore isoprene (with $\tau_c > 600$ s) is transported through a locally variable field of OH which is influenced by the solar actinic flux and additional reactants like NO_2, NO, CO, CH_4 and various volatile organic compounds (VOCs). Note that for these considerations the Damköhler number is used as a timescale for the chemical reactant isoprene with respect to the active species (OH) and is no longer a timescale of a specific reaction.

Such atmospheric chemical systems were analysed by model studies of Verver et al. (2000) and van Stratum et al. (2012) for isoprene in a complex chemical mixture and its behaviour in the complete ABL and by Patton et al. (2001) for isoprene in a mixture with CO but analysing the influences of emission, mixing and reaction on the intensity of segregation I_S within and directly above an idealised deciduous forest. Both analyses found $I_S < 0$ near the bottom of their model areas indicating that the reaction (isoprene + OH) imposes a negative correlation between both compounds. Patton et al. (2001) applied LES and specified terms in the balance equation for isoprene with the largest influence on fluxes and I_S.

Recently Ouwersloot et al. (2011) also applied LES to study how convection and turbulence above a differentially heated land surface representing alternating forest and savanna areas influence I_S for the isoprene–OH reaction. In this study, buoyant production and their differences between both surface types as well as inhomogeneous emission source strength cause changes in I_S. As in the study by Patton et al. (2001), the modelled chemical reactions are for low NO_x conditions where the major sink for OH is isoprene. Their chosen relations of friction velocity u_* to convective-scale velocity w_* with $u_* < w_*$ or $u_* \ll w_*$ represent convective to free convective conditions (Stull, 1988).

Also recently Pugh et al. (2011) applied results from the field study ECHO 2003 (Dlugi et al., 2010) to estimate a potential influence of segregation for this reaction on results of another field study above a tropical rain forest area. In addition, Butler et al. (2008) estimated that they need values of $-0.6 \le I_S \le -0.3$ to interpret their chemical measurements with an aircraft in the ABL during the GABRIEL field

campaign also above comparable vegetation types, but after an extended error analysis estimated $I_S \approx -0.13$.

The influence of inhomogeneous mixing on the reaction of isoprene with OH above a deciduous forest canopy was investigated by Dlugi et al. (2010) using highly time-resolved data of OH and isoprene measured during the experiment ECHO 2003 (Emission and CHemical transformation of biogenic volatile Organic compounds).

They obtained $-0.15 \leq I_S \leq 0$ for this reaction from the first direct analysis of field data above a deciduous mixed forest. Their data are mostly for $u_* \gtrsim w_*$, variable NO_x with $NO_x > 3$–4 ppb in the morning and significantly decreasing values around 10:00 CET and later on, but highly variable photolysis rates. In general an upward-directed isoprene flux was determined. But occasionally, downdrafts with negative vertical mean velocity $\overline{w}$ and negative turbulent isoprene fluxes were observed. In addition, some time intervals of this field study were also characterized by $u_* < w_*$, which allows a comparison with modelled results for convective conditions.

The present work extends the study by Dlugi et al. (2010) and investigates the influence of chemistry and different mixing and transport processes on the effective reaction rate for isoprene with OH. The measurements used in this paper were first published by Dlugi et al. (2010) showing that the data set – although it is limited by the short time measuring phase – is still unique and, therefore, is used to derive meaningful results like vertical fluxes and segregation intensity I_S of isoprene and HO_x radicals above a forest. The same data set is now applied to further evaluate which chemical and dynamical processes are responsible for the observed segregation. To find general relations between the segregation intensity I_S and these processes, the balance equation of the covariance $\overline{c_i' c_j'}$ is taken as a frame to analyse the field data. Such an approach was applied for example by Lenschow (1982) to analyse interactions between chemistry and transport in the ABL for the $NO-NO_2-O_3$ system. From this, an equation for I_S is derived, to relate I_S to the three controlling terms which quantify the influences of transport and mixing as well as chemical reactions. A short description of the ECHO experiment is given in Sect. 2 with additional details given in the Supplement. Sections 3–5 present an analysis of the balance equations of the mixing ratio of isoprene, the covariance of mixing ratio between isoprene and OH and the segregation intensity for the reaction between isoprene and OH.

The results in Sects. 3 and 4 show that findings from the ECHO study agree qualitatively with results of the modelling study by Patton et al. (2001) with respect to a relationship between I_S and OH reactivity in a chemical system composed of isoprene, as well as NO_2, NO, CO, CH_4 and various VOCs. Such a relation between I_S and OH reactivity can only be established if available OH for the reaction with isoprene is modelled based on the measured mixing ratios of OH_{meas}. The modelled OH_{mod} shows a better correlation

with I_S than with OH_{meas}. It can be also shown that the absolute value of the segregation intensity $|I_S|$ increases with increasing normalised variance (or standard deviation) of isoprene, although additional factors are of influence during the field experiment.

We also discuss the empirical relations found for the correlation coefficient r_{ij} between isoprene and OH and some parameter like the mean reaction rate $k_{ij} \times \overline{c_i} \times \overline{c_j}$ (see Table A1).

In addition a new diagnostic equation for the covariance of chemical compounds $\overline{c_i' c_j'}$ between isoprene (index i) and OH (index j) is formulated in Sect. 5. An order of magnitude analysis of terms of the balance of the covariance $\overline{c_i' c_j'}$, which significantly influences sign and magnitude of I_S, is presented. The following discussion shows that also a new diagnostic equation for I_S can be formulated and applied to the analysis of ECHO 2003 data from 25 July 2003 (Dlugi et al., 2010). In the last sections we focus on the different terms of the balance equation influencing the covariance between isoprene and OH as well as I_S and compare the results from the field with findings from model predictions especially by Patton et al. (2001) and Ouwersloot et al. (2011).

2 The ECHO 2003 field study

2.1 Field site and measurements

In 2003 the ECHO intensive field campaign was performed from 17 June to 6 August. Three towers were installed in a mixed deciduous forest with dominating tree species beech, birch, oak and ash, and a mean canopy height $h_c = 30$ m. The vertically integrated one-sided leaf area index in a radius of 50 m around the main tower varied between 5.5 and 5.8. The towers were aligned parallel to the main wind direction (Schaub, 2007) with the main tower in the centre. The west tower had a distance of 220 m from the main tower, and the east tower was located 120 m away. This, for example, allowed the investigation of the influence of the spatial distribution of biogenic volatile organic compound (BVOC) sources (isoprene, monoterpenes) on measured fluxes (e.g. Spirig et al., 2005). The field measurements were supported by the physical modelling of this forest site in a wind tunnel (Aubrun et al., 2005) also to estimate the influences of spacial heterogeneity of emission sources on measured fluxes of some BVOCs. All measurements reported in the present paper were obtained on 25 July from 09:00 to 15:00 CET on the main tower. The main tower with a height of 41 m, and the upper measuring platform at 36 m, was equipped with nine sonic anemometers/thermometers (METEK, instrument type: USA-1; time resolution 10 Hz) between 2 m and 41 m, and eight psychrometers (dry and wet bulb temperatures) at the same heights except 41 m. A time resolution for air temperature T and specific humidity q of 15 s could be achieved. Radiation quantities and photolysis frequencies

were obtained by radiometers directly above the canopy (h_c=30 m) with a time resolution of 3 s (Bohn et al., 2004; Bohn, 2006; Bohn et al., 2006). Occasionally vertical profiles were measured.

OH and HO_2 radical concentrations were measured by LIF (Holland et al., 1995, 2003) on a vertically movable platform. For the reported measurements it was positioned above the canopy, with the inlet at 37 m height (Kleffmann et al., 2005). A proton-transfer-reaction mass spectrometry (PTR-MS) instrument for measurement of isoprene, monoterpenes, methyl venyl ketone (MVK) and methacrolein (MACR) was installed at the ground, using a sampling line to collect air at the height of the ultrasonic anemometer (Ammann et al., 2004; Spirig et al., 2005). The distances of the inlets of the PTR-MS and LIF instruments from the ultrasonic anemometer measuring volume were 0.45 m and 0.6 m, respectively. This spatial arrangement requires corrections to the calculated fluxes as is outlined by Dlugi et al. (2010) and given again in the Supplement. For all aspects identical to the procedures as applied by Spirig et al. (2005), we refer to their work. Aspects which we handled in a different way are described in more detail in the Supplement. The mean meteorological conditions above the canopy are presented in the Figs. S1–S3 of the Supplement together with the friction velocity as a measure of mechanical turbulence as in Dlugi et al. (2010).

2.2 Summary of some results

During the ECHO campaign, a feasibility study was performed on 25 July 2003 (day 206 of year 2003) to measure fluxes and covariances not only for isoprene but also for the first time for OH and HO_2 radicals. The measurements took place in the time period between 09:00 and 15:00 CET. This period is characterized by cloudy conditions (Fig. S1 in Supplement) with a moderate horizontal wind velocity variation (Fig. S3 in Supplement) and slightly unstable to neutral stratification above the canopy. Broken clouds caused significant fluctuations of all radiation quantities above canopy, as is shown for the net radiation, Rn, and $J(O^1D)$ in Fig. S1 in the Supplement. The air temperature T increased from 19 to 26.5 °C, while the specific humidity q increased only slightly from 09:00 to 12:00 CET up to about 9.5 g kg^{-1} and then decreased to about 8 g kg^{-1} (Fig. S2 in the Supplement). The variability of solar radiation is reflected in the correlated low-frequency variations of OH on a timescale of 10 min to 30 min (Figs. S4 and S5 in the Supplement), which can be explained by the primary, photochemical production of OH (Kleffmann et al., 2005). The measured HO_2 behaves differently compared to OH (Fig. S6 in the Supplement) and increases stepwise following the temperature record (Fig. S2 in the Supplement). Temperature ramp-like structures (Fig. S2 in the Supplement) occurred after 09:30 CET, when net radiation peaked (Fig. S1 in the Supplement) and wind turned to a sector from SW to SE,

in parallel to maxima in HO_2 (Fig. S6 in the Supplement) and isoprene (Fig. S8 in the Supplement). The arithmetic mean values of the ratio $(MVK + MACR)/$ isoprene $= 0.52$ at 09:00–12:00 CET and 0.26 at 12:00–15:00 CET hint towards a changing influence of photochemical processes and advection, but are at the upper end of data obtained at daytime by Schaub (2007) and Spirig et al. (2005). Following the discussion by Schaub (2007), this result suggests that the residence times of BVOCs in the canopy atmosphere are longer than 20 min.

Most points of the highly time-resolved data and all time-averaged mean values of OH and HO_2 concentrations are above the detection limits (Fig. 1). The same holds for temperature, humidity, and vertical velocity as well for the organic compounds as discussed by Dlugi et al. (2010). For both radicals, the standard error Δa is below 10 % of their arithmetic means, and the relation $\sigma_x/\overline{x} < 0.42$ holds for each 10 min interval. The latter relation suggests also that Taylor's hypothesis is valid for these chemical species (Stull, 1988) but not always for isoprene. Skewness (Sk) as well as kurtosis (Kur) point towards near normally distributed data (but still with deviations from it) for radicals with Sk ≈ 0 and Kur ≈ 3. This is not the case for $J(O^1D)$ which shows a significant deviation from the characteristics of a normal distribution. The covariance between $J(O^1D)$ and OH is always positive with only small correlation coefficients, $r \leq 0.5$, and even two intervals with $r \approx 0$ on a timescale up to 10 min. This is in contrast to the lower-frequency OH variations occurring on a timescale of 10 min to 30 min, which are well correlated with $J(O^1D)$ (cf. Supplement Figs. S1 and S5).

Other quantities like vertical wind velocity w, temperature T and organic compounds mainly show a different statistical behaviour with respect to the higher moments Sk and Kur (Dlugi et al., 2010).

Most of the w data are still near normally distributed, but occasionally show values with Kur ≥ 4. Temperature data show Sk > 0 until about 13:40 CET, with a number of events with Kur > 4. This hints towards a more peaked distribution than a normal distribution in atmospheric turbulence (Hollinger and Richardson, 2005), but with a large number of data points (Sk > 0) smaller than the arithmetic mean, especially for T until 13:40. Comparable results with Sk > 0 are obtained for BVOCs with more data points smaller than the arithmetic means and even more peaked distributions (Kur > 4) during some periods. The third and fourth moments Sk > 1 and Kur > 4 are found only in time intervals with lower mixing ratios. Comparing the statistics for w and trace substances in most 10 min intervals, the small values below the mean occur simultaneously. Note that homogeneously mixed conditions are characterized by Sk ≈ 0 and Kur ≈ 3 (e.g. Wahrhaft, 2000). Therefore, one might also expect some deviation of the segregation term from $I_S = 0$, at least for the system OH + isoprene.
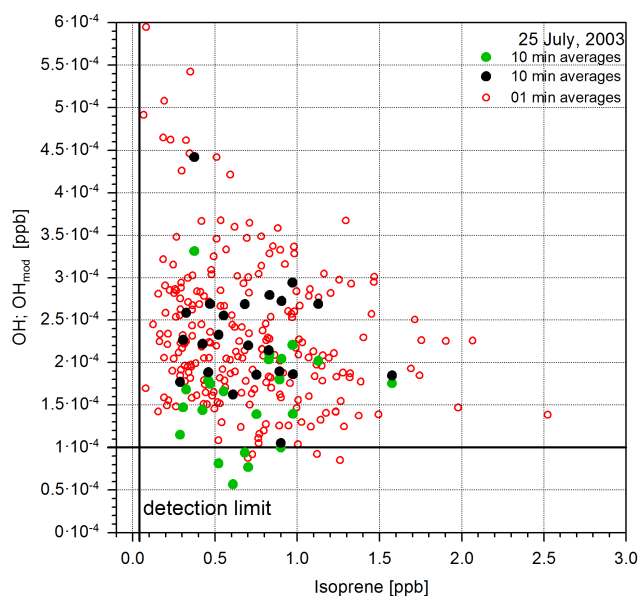
Figure 1. The relation between mixing ratios of isoprene and OH (25 July 2003, 09:00–15:00 CET). The detection limit ($S/N = 2$) of the LIF instrument is 0.1 ppt for OH and of the PTR-MS 41 ppt for isoprene at a measuring frequency up to 0.2 Hz (Dlugi et al., 2010). The results for three time average intervals are given with the green dots for OH_{mod}.

2.3 Relationship between OH and isoprene

The 1 min averaged mixing ratios of OH and isoprene show a large scatter (Fig. 1, Supplement Figs. S5, S8) caused by atmospheric variability of the OH concentration and instrumental noise. An inverse relationship between OH and isoprene should be observed in an atmosphere where the reaction between OH and isoprene is the dominating loss process for OH. For the time-averaged 10 min data, only some points remain in Fig. 1 which follow qualitatively such a relation. Especially in the morning, OH has a number of other chemical sinks than isoprene (Table 1 and Figs. S15–S18 in the Supplement). Most of these data are from vertical profile measurements (e.g. Schaub, 2007), and only half-hourly results are available. While NO_2 decreases with time, the mixing ratios of CO and CH_4 stay nearly constant. To further analyse the reaction between OH and isoprene and to evaluate the influence of segregation, it is essential to specify the OH available for this reaction.

This is done following the concept (Eq. 1) that measured OH can be expressed by the influences of production $P(OH)$ and loss $L(OH)$ (Seinfeld and Pandis, 1997). Here $L(OH)$ is equal to the OH reactivity.

We formulate an equation (Eq. 4) to estimate a factor f to calculate the isoprene sink relative to the sink by other compounds for the reaction with measured OH(meas). From measurements during ECHO 2003 the mixing ratios of NO, NO_2, CH_4, CO, sum of monoterpenes and also OH and iso-

prene are known (Table 1). For stationary conditions Eq. (1) is valid:

$$OH_{meas} = \frac{production}{loss} = \frac{P}{L} = \frac{P}{\sum_{l=1}^{N} k_{lj} \times \overline{c_l}}. \quad (1)$$

Here index j is for OH while index l is for any chemical compound with an average concentration $\overline{c_l}$ reacting with OH. Therefore one may formulate

$$\overline{L} = k_{ij} \times \overline{ISO} + \sum_{l=1}^{N-1} k_{lj} \times \overline{c_l} \quad (2)$$

to separate the OH loss by isoprene (index i) from those of other compounds (Tables 1 and 2). With Eq. (1) and division by the sum term in Eq. (2), we obtain

$$\overline{OH_{meas}} \times \left(\frac{k_{ij} \times \overline{ISO}}{\sum_{l=1}^{N-1} k_{lj} \times \overline{c_l}} + 1 \right) = \frac{\overline{P}}{\sum_{l=1}^{N-1} k_{lj} \times \overline{c_l}}$$

$$= \frac{\overline{P}}{\overline{L} - k_{ij} \times \overline{ISO}}. \quad (3)$$

Finally one obtains for a diagnostically modelled OH mixing ratio OH_{mod} with $c_l > 0$ and $N > 1$:

$$\overline{OH}_{mod} = \overline{OH}(meas) \left(\frac{k_{ij} \times \overline{ISO}}{\sum_{l=1}^{N-1} k_{lj} \times \overline{c_l}} \right) = \overline{OH} \times f$$

$$= \frac{k_{ij} \times \overline{ISO}}{\overline{L} - k_{ij} \overline{ISO}} \times \frac{\overline{P}}{\overline{L}}. \quad (4)$$

Here we use $c_j = OH_{meas} = OH$ as otherwise in the text. The factor f is also called the fraction of isoprene reactivity to total reactivity or the branching ratio of the reaction between isoprene and OH relative to the reactions of OH with all other compounds.

The influence of different chemical compounds on f is given in Tables 1 and 2. Not all compounds influencing $\overline{L}$ are available from measurements. Note that if all other compounds influencing $L(OH)$ are considered, one obtains $f > f$ (all reactants). But one can estimate the impact of other reactants on our results, because most compounds of known large influence are considered. As only half-hourly and hourly values are available from vertical profile and concentration measurements for compounds NO_2, NO, CO and CH_4 in Tables 1 and 2, the time resolution for the calculation of factor f is limited. The possible influence of short time fluctuations of mixing ratios on f is discussed later on.

The modelled OH mixing ratio shows only a slightly better inverse relationship to the isoprene mixing ratio (Fig. 1).
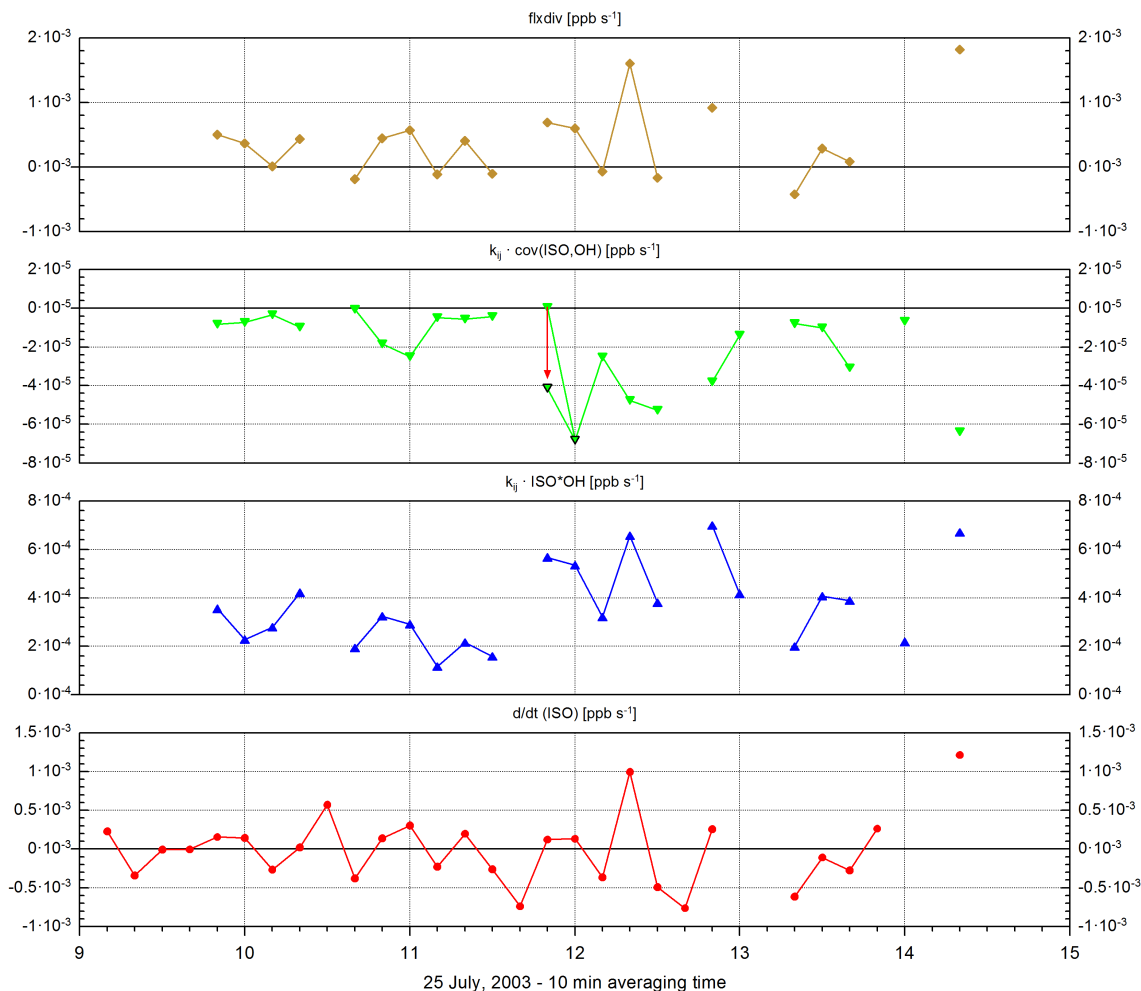
3 Balance of the mixing ratio

3.1 Balance equation

The balance equation Eq. (5) for the mixing ratios of trace gases is widely used to discuss the role of chemical reactions

Table 1. Mean mixing ratios on 25 July 2003 (day 206) at the ECHO site.

Time period (CET)	Unit	09:00–10:30	10:30–11:30	11:30–13:00	13:00–15:00
NO_2	ppb	> 2.5	2.0–2.5	1.8–2.1	1.1–1.8
NO	ppb	> 0.75	0.6–0.95	0.4–0.8	0.2–0.5
CO	ppb	> 150	> 140	> 140	> 140
CH_4	ppb	$\simeq$ 1800	$\simeq$ 1800	$\simeq$ 1800	$\simeq$ 1800
Isoprene	ppb	0.5–0.7	0.3–0.7	0.3–1.13	0.45–1.58
$\sum$ Monoterpenes	ppb	0.13–0.27	0.21–0.32	0.2–0.34	0.23–0.30
O3	ppb	19–25	25–30	30–35	35–39

Figure 2. The four terms of the balance equation for the mixing ration of isoprene (Eq. 5) calculated according the finite difference method as described in the text. The correction of the covariance is explained in Sect. 5.3.4

on fluxes of reactive compounds (e.g. Lenschow, 1982; Vilà-Guerau de Arellano et al., 1995; Kramm et al., 1995; Dlugi et al., 2010). This equation has two terms (the covariance and the product of mean mixing ratio) which compose I_S (see Eq. 7).

The basic concept and formulation of Eq.(5) is discussed by Kramm and Meixner (2000) and Dlugi et al. (2010). As air

temperature (see Fig. 6b in Dlugi et al., 2010) and pressure show only small changes during the measuring time on day 206 of year 2003 from 9:00 to 15:00 CET of the ECHO study, the variation of mixing ratios with time is almost comparable to the variation of partial densities or concentrations. In a simplified version, neglecting horizontal advection, Eq. (5)

Table 2. Mean reaction rates [s^{-1}] for different reactants, the total OH loss $L(OH)[s^{-1}]$, the OH reactivity and the percentage of OH reacting related to isoprene for 25 July 2003 at the ECHO site.

Time (CET)	09:00–10:30	10:30–11:30	11:30–13:00	13:00–15:00
ISO	1.76–0.88	1.61	1.78	2
NO$_2$	> 1	0.78	0.67	0.45
NO	0.07	0.06	0.03	0.02
CO	0.9	0.84	0.84	0.84
CH$_4$	0.28	0.28	0.28	0.28
$\sum$ Monoterpenes	< 0.68	0.51	0.55	0.5
%	30–60	65	75	≈ 95
$L(OH)$	4.69	4.08	4.15	4.09
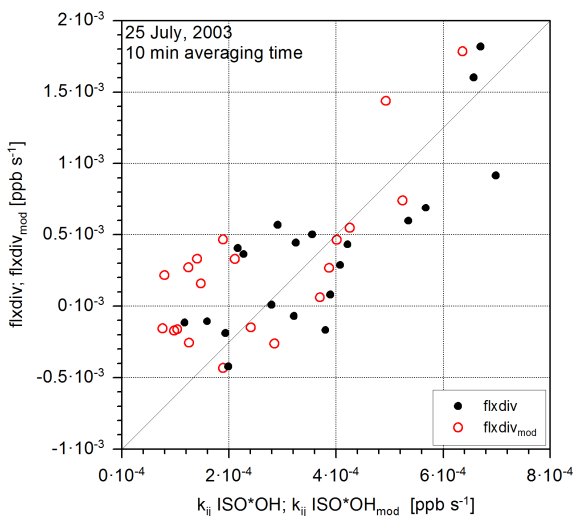
Figure 3. The residual flux divergence from Eq. (5) as a function of the mean reaction rate for OH and OH$_{mod}$.

reads

$$\frac{\partial \overline{c_i}}{\partial t} = -\frac{\partial}{\partial z}(\overline{w} \times \overline{c_i} + \overline{w'c_i'}) - k_{ij}(\overline{c_i} \times \overline{c_j} + \overline{c_i'c_j'}), \quad (5)$$

where index i represents isoprene, index j here represents OH, $\overline{c_i}$ and $\overline{c_j}$ are the mean values of mixing ratios of reactive components i and j, $\overline{w'c_i'}$ is vertical turbulent flux (here of isoprene), k_{ij} is the reaction rate constant, and $\overline{c_i'c_j'}$ is the covariance between reactants caused by turbulent fluctuations of both compounds. $\bar{w} \cdot \overline{c_i}$ is the vertical advective flux with the mean vertical velocity (see also Table A1: list of symbols).

Here the divergence of the sum of the turbulent flux and the vertical advective flux is the residuum which also summarises all other influences of horizontal advection as discussed in the following section and in Sect. S3 in the Supplement. It can only be estimated from point measurements at the main tower and the west tower, the physical modelling by Aubrun et al. (2005) and the calculation of footprints for the isoprene flux at both towers based on the distribution of emission sources (Figs. S19–S21 in the Supplement).

The time derivative on the left side of Eq. (5) is called "storage term" (e.g. Stull, 1988), and the first term on the right side is the "flux divergence" of the sum of the vertical advective and turbulent isoprene fluxes which can be itself either negative or positive. The second term on the right side is the chemical reaction term composed of the product k_{ij} with the product of mean mixing ratios as well as the covariance. In this analysis $c_j = OH$ is considered as the only reactant of isoprene $c_i = ISO$. As explained in Appendix A of Dlugi et al. (2010), any emission flux of trace gases is introduced into this differential equation by boundary conditions when integrating over the vertical z coordinate. Rearranging the terms in Eq. (5) for $c_i =$ isoprene allows the estimation of the vertical divergence of the sum of the advective and turbulent fluxes as a residuum caused by the influences of the chemical reaction term and the storage term. As discussed in Sects. 3 and 4 in the Supplement, this residuum includes also all contributions from advection with the mean horizontal flow. For ECHO 2003, this residuum is calculated for the reaction of isoprene with OH (Dlugi et al., 2010) with

$$k_{ij} = \frac{170}{T} e^{\frac{409}{T}} \text{ [ppb}^{-1}\text{s}^{-1}], \quad (6)$$

where T is in K. Equation (5) is applied for a reaction R = isoprene + OH and day 206 (25 July 2003) of ECHO 2003 at height $z = 37$ m for the main tower for the data set as described in Dlugi et al. (2010) and presented there in Figs. 5a and 6a–c. The temperature for the time period from 09:00 to 15:00 CET (see Supplement Fig. S3) increases from 292 to 298 K, which causes a variation in Eq. (6) of only 4.7 % in k_{ij} (e.g. from 2.36 ppb^{-1} s^{-1} to 2.25 ppb^{-1} s^{-1}). Therefore, a mean value $k_{ij} = 2.3$ ppb^{-1}s^{-1} is used for further analysis.

3.2 Results for the balance of mixing ratio

For the analysis of the isoprene mixing ratio balance, the mean values and covariances calculated from 10 min time intervals as described in the Supplement in Sect. S2 and by Dlugi et al. (2010) are considered. The terms of Eq. (5) can
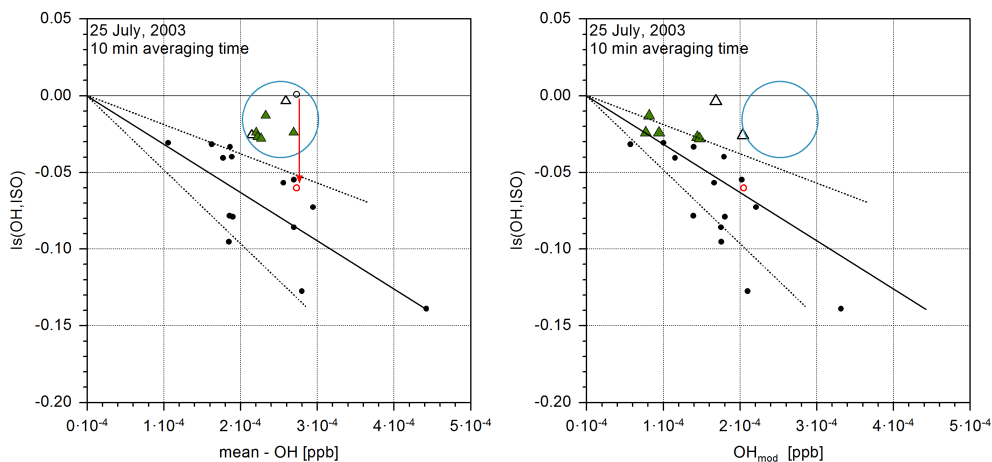
Figure 4. The intensity of segregation I_S as a function of the measured mean OH mixing ratio with a relation proposed according to model calculations of Patton et al. (2001) (solid line). The sector between the dotted lines encloses a range of $\pm 40\%$ around the solid line. Left part: data points outside this relation are within the blue circle. Right part: I_S as a function of the modelled OH_{mod} and OH – loss as given in Table 2 for mean mixing ratios of Table 1. The arrow gives the corrected value according to Sect. 5.3.4.
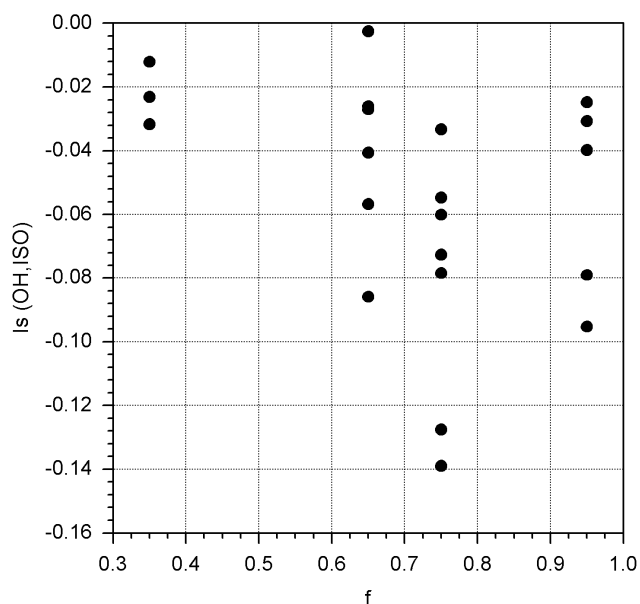

Figure 5. The intensity of segregation I_S as a function of factor f from Eq. (4) with data from Tables 1 and 2.

be calculated replacing the differential in the storage term by a time difference Δt and the arithmetic mean of quantities at time steps t_k and t_{k+1} (Press et al., 1991).

The chemical reaction term splits into two parts with the first, positive part being larger than the negative covariance term by about an order of magnitude (Fig. 2). Note that the corresponding time series of OH and isoprene (see Supplement Figs. S5, S8 and in Dlugi et al., 2010) show gaps when the calibration procedures were applied. These gaps appear

even more pronounced in the time series of 10 min averages (Fig. 2).

The first term – the storage term – varies between about $\pm 10^{-3}\,\mathrm{ppb\,s^{-1}}$ and zero. The resulting flux divergence is dominated by this term and the first term of the chemical reaction term with contributions of the covariance term smaller by up to an order of magnitude. A residual positive isoprene flux divergence is partly related to the loss by reaction with OH during vertical transport. Note that the flux divergence itself is negative, but the residuum in general becomes positive by the negative sign in Eq. (5).

The covariance term in the reaction term is negative and reduces the contribution of the reaction term to the flux balance by up to 10% because its absolute magnitude is significantly smaller than the product of the mean values. The neglect of horizontal advection may not be strictly valid (e.g. Sun, 2007). Therefore, the determination of the flux divergence – in the mathematical sense as a residuum – summarises also all unknown contributions of horizontal advection (Supplement Sect. S3). The relation of the "residual flux divergence" and the product of the mean values of isoprene and OH times k_{ij} (the mean reaction rate) is linear with a correlation coefficient $r = 0.81$ (Fig. 3).

The relation between the flux divergence and the covariance of the reactants (not given) shows some more scatter ($r = 0.60$) with increasing values for more negative covariances. Negative values of the "flux divergence" are caused by the storage term because both terms are of the same order of magnitude. The chemical reaction terms are always smaller. Therefore chemistry influences the total residual flux divergence to a lesser extent than turbulent mixing and advection (as well as convection) with the mean flow. If the calculation is performed for $\overline{OH}_{mod}$ instead of $\overline{OH}$, the results show a lesser dependence of the residual
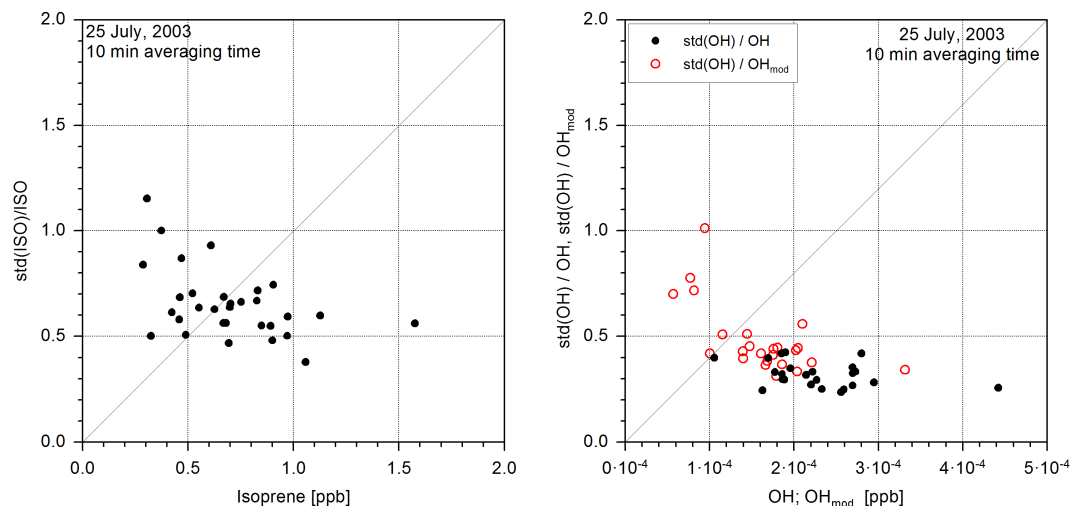
Figure 6. The normalised standard deviations of isoprene and OH (OH$_{mod}$) vs. their mixing ratios.
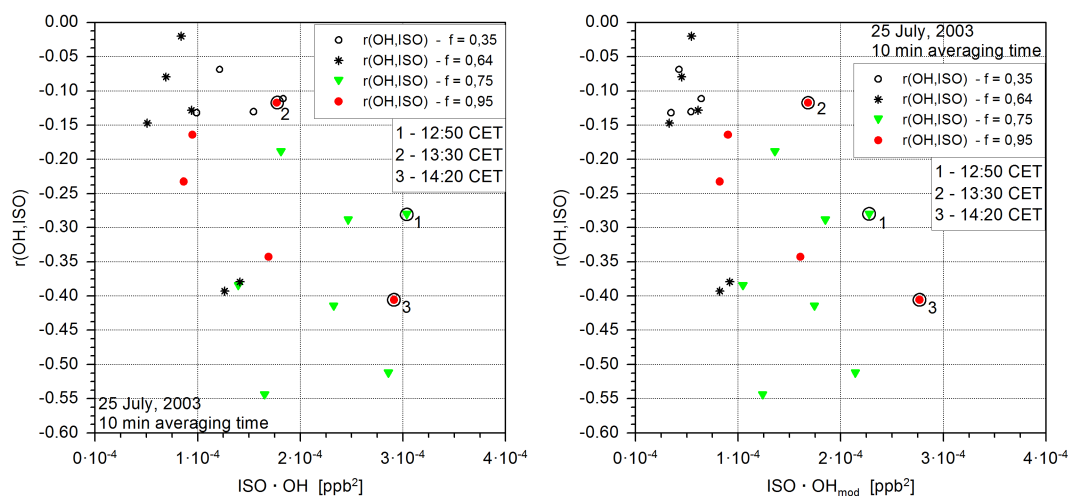

Figure 7. The correlation coefficient between isoprene and OH respectively OH$_{mod}$ as a function of the product of mean mixing ratios with the three points as discussed in Sects. 4.2.4 and 4.2.5.

flux divergence on the mean reaction rate. Note that if the influences of changing photolysis frequency and inhomogeneous mixing for the covariance at 11:50 CET are separated from each other, the data point at cov(Iso, OH) $\simeq 0$ and flux divergence 6.8×10^{-4} ppb s^{-1} in Fig. 2 is shifted to a covariance of -1.8×10^{-5} ppb^2 respectively a value of $2.3 \times (-1.8 \times 10^{-5})$ ppb^{-1} s^{-1} = -4.14×10^{-5} ppb^{-1} s^{-1}. The relation between the two parts of the reaction term is the intensity of segregation and is discussed in the following.

4 Segregation intensity

4.1 Introduction

The segregation intensity I_S (Eq. 7) for bimolecular reactions is defined as the covariance $\overline{c_i' c_j'}$ of reactant mixing ratios c_i

and c_j divided by their mean values $\overline{c_i}$ and $\overline{c_j}$ (e.g. Danckwerts, 1952; Damköhler, 1957; Vilà-Guerau de Arellano and Lelieveld, 1998) and is given for the system of c_i = isoprene and c_j = OH by

$$I_S = \frac{\overline{c_i' c_j'}}{\overline{c_i} \times \overline{c_j}}. \tag{7}$$

Any covariance can be also presented by the product of the standard deviations σ_i and σ_j times the specific correlation coefficient r_{ij} (Eq. 8) (e.g. Sachs and Hedderich, 2006).

$$\overline{c_i' c_j'} = r_{ij} \times \sigma_i \times \sigma_j \tag{8}$$

Therefore, if $\overline{c_i' c_j'} \simeq 0$ in Fig. 2, $r_{ij} \simeq 0$, the correlation between the turbulent field quantities c_i' and c_j' vanishes
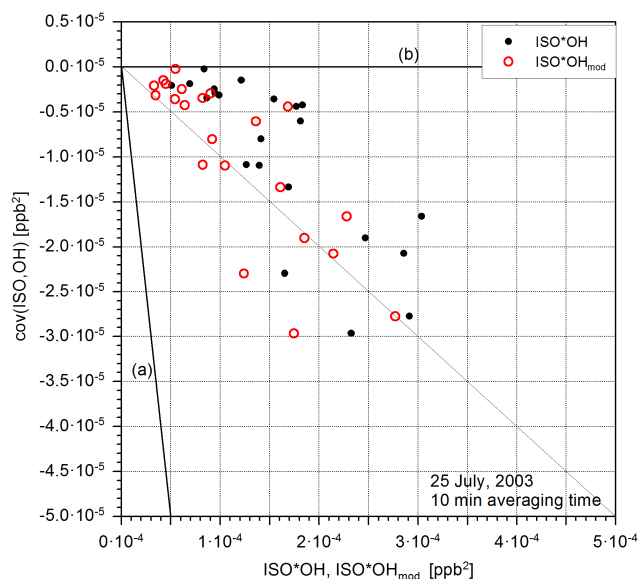
Figure 8. The covariance between isoprene and OH calculated as explained in the text as a function of product of means. The two lines **(a)** and **(b)** are explained in the text (Sect. 4.2.4). The covariance between isoprene and OH calculated as explained in the text as a function of product of means.

Figure 9. The correlation coefficient between isoprene and OH as a function of segregation intensity I_S.

because $\sigma_i > 0$ and $\sigma_j > 0$ is valid. Inserting Eq. (8) – as discussed in the Supplement – into Eq. (7) shows that the product of the normalised standard deviations of both reactants has to be multiplied by their correlation coefficient.

4.2 Results for the segregation intensity

4.2.1 Relation to mean OH mixing ratio

The measured OH and isoprene concentrations show only a qualitative inverse relationship (Fig. 1), which is plausible since the reaction with isoprene is not the only dominant OH loss (Tables 1, 2). The superimposed scatter in the correlation plot (Fig. 1) has several reasons. It is partly due to instrumental noise in the measurement of OH and isoprene (Dlugi et al., 2010), partly due to additional OH loss by other compounds (e.g. NO_2, NO, CO, CH_4, VOCs) and variations in the chemical production of OH (e.g. photolysis of ozone and HONO Bohn et al., 2004; Bohn, 2006; Kleffmann et al., 2005). Note that an inverse relationship is comparable to the prediction by Patton et al. (2001) and Pugh et al. (2011), who assumed an inverse dependence of OH on isoprene in a mainly isoprene-dominated atmosphere.

The relation between I_S and the mean OH mixing ratio in Fig. 4 (left) shows that part of the data follow a negative correlation of I_S with $\overline{OH}$, a result also expected by a modelling study by Patton et al. (2001) if their definition of Damköhler number $D_c = \tau_t \times k_{ij} \times \overline{OH}$ (with the notation as in this paper) is applied. A comparable presentation is given for ECHO 2003 in Fig. 4 with a linear fit through the origin
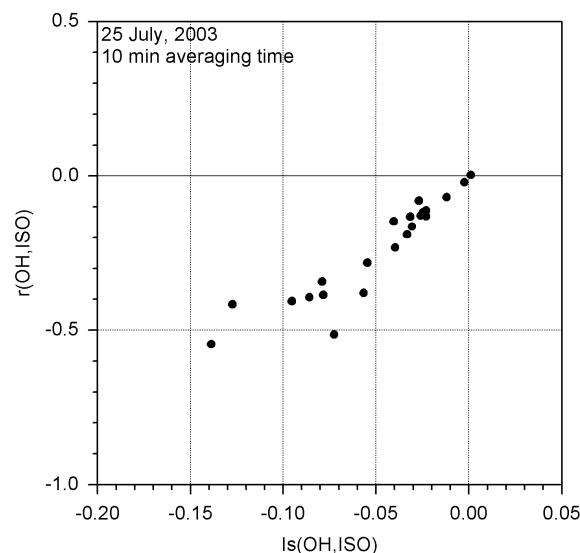
with a variability of $\pm 40\%$ marked by the dotted lines. In the left part of Fig. 4 some data points are outside in a separate cluster for a range of $I_S < -0.025$ which corresponds to situations with only a small correlation coefficient between isoprene and OH being determined by Eq. (8).

(Note also that one point at $I_S \simeq 0$ and $\overline{OH} = 2.7 \times 10^{-4}$ ppb is shifted to $I_S = -0.06$ by the same effect discussed for the covariance (see Sect. 5.3.4).)

These data points (in the circle) are from measuring periods with neutral to slightly unstable stratification and mixing ratios of NO_2, NO and also CO higher than at other times as given in Table 1 (see also Supplement Figs. S15–S17). For these conditions additional chemical sinks act more effectively on mean OH, and, therefore, the relative amount of OH consumed by isoprene, OH_{mod}, decreases (Table 2). In contrast, the data points within the dotted sector in Fig. 4 are for a reduced influence of other chemical sinks for OH.

The measured mean OH mixing ratio is nearly constant between 09:50 and 12:10 CET and reaches a maximum around 12:30 CET with a small decrease below the morning values after 12:50 CET. The maximum is for a maximum in ozone photolysis frequency $J(O^1D)$ (see Supplement Figs. S1, S5, S6) and the decline for a decrease of $J(O^1D)$ on average with some maxima in between. The different contributions of isoprene and other compounds given in Table 1 to the loss of OH, $L(OH)$, is estimated for four time periods (Table 2). The mean fraction f of isoprene contribution to $L(OH)$ is calculated (Table 2, Fig. 5) according to the concept described in Sect. 2.3. $L(OH)$ has a maximum in the first period, a secondary maximum in the third period, where the contribution of ozone photolysis to the production term $P(OH)$ reaches a maximum, and comparable values with $L(OH) \approx P(OH)$ above $4\,s^{-1}$ otherwise. But the relative contribution
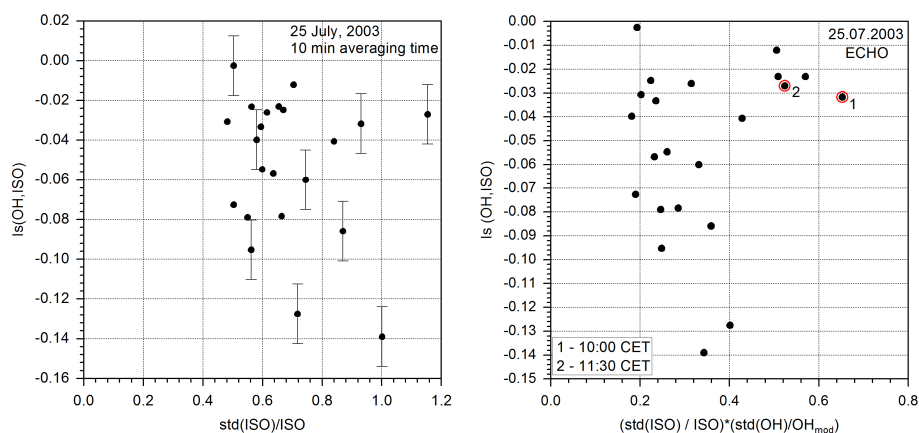
Figure 10. The dependence of the intensity of segregation on isoprene standard deviation (left) and normalised variance (right). The specific conditions for the red marked points are described in Sect. 4.2.5.
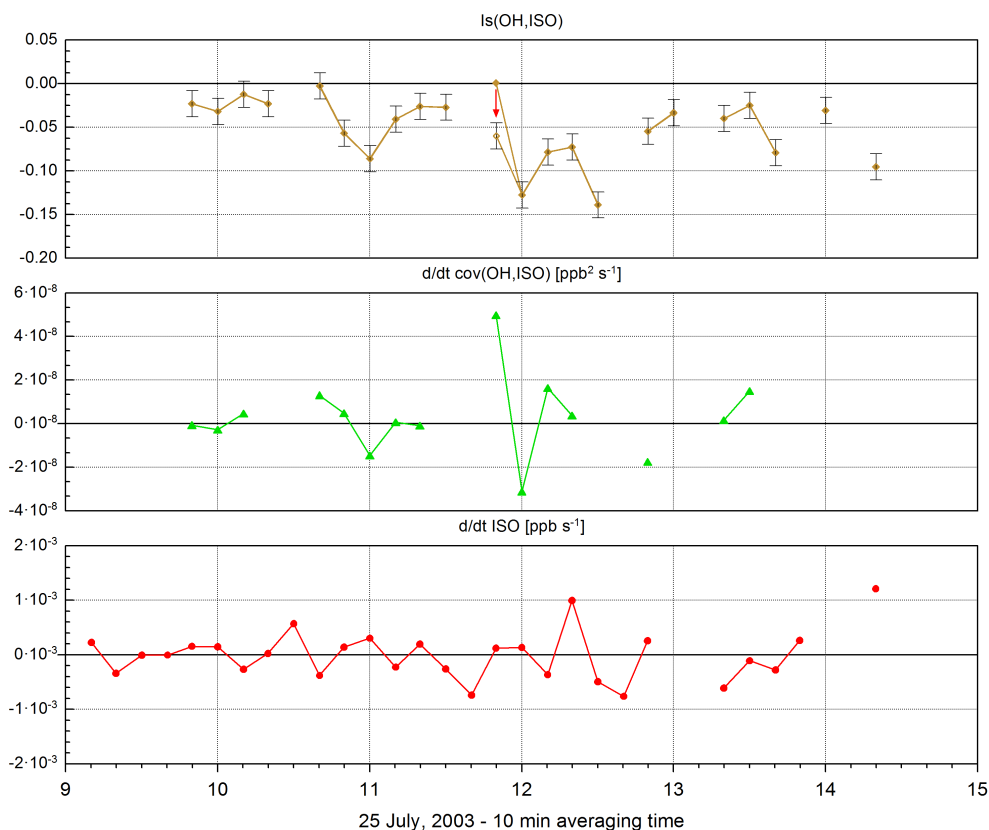

Figure 11. The storage term for the covariance between isoprene and OH from Eq. (9) compared to the storage terms of the balances of isoprene (Eq. 5) and the intensity of segregation I_S as given by Dlugi et al. (2010) with the corrected data point (Sect. 5.3.4).

of isoprene to $L(\mathrm{OH})$ increases significantly over the measuring period. Therefore in the presentation of the segregation intensity I_S vs. $\mathrm{OH}_{\mathrm{mod}} = f \times \mathrm{OH}_{\mathrm{meas}}$ in the right panel of Fig. 4, all data points residing originally in the blue circle move to the left. With the exception of two of them at 10:40 CET and 13:30 CET, all values move to the area within the dotted lines. The largest effect (see also Fig. 5) is found

for time periods before 10:30 CET with $f \leq 0.6$. Note that f vanishes in I_S because f contributes to both terms in Eq. (7). The same holds for the correlation coefficient r_{ij}, but not for the mean reaction rate or the covariance itself. Comparing the results in Fig. 5 with Fig. 4, the factor f acts on the complete range of segregation intensity. But the largest values of I_S are determined for the smallest f. This suggests that not
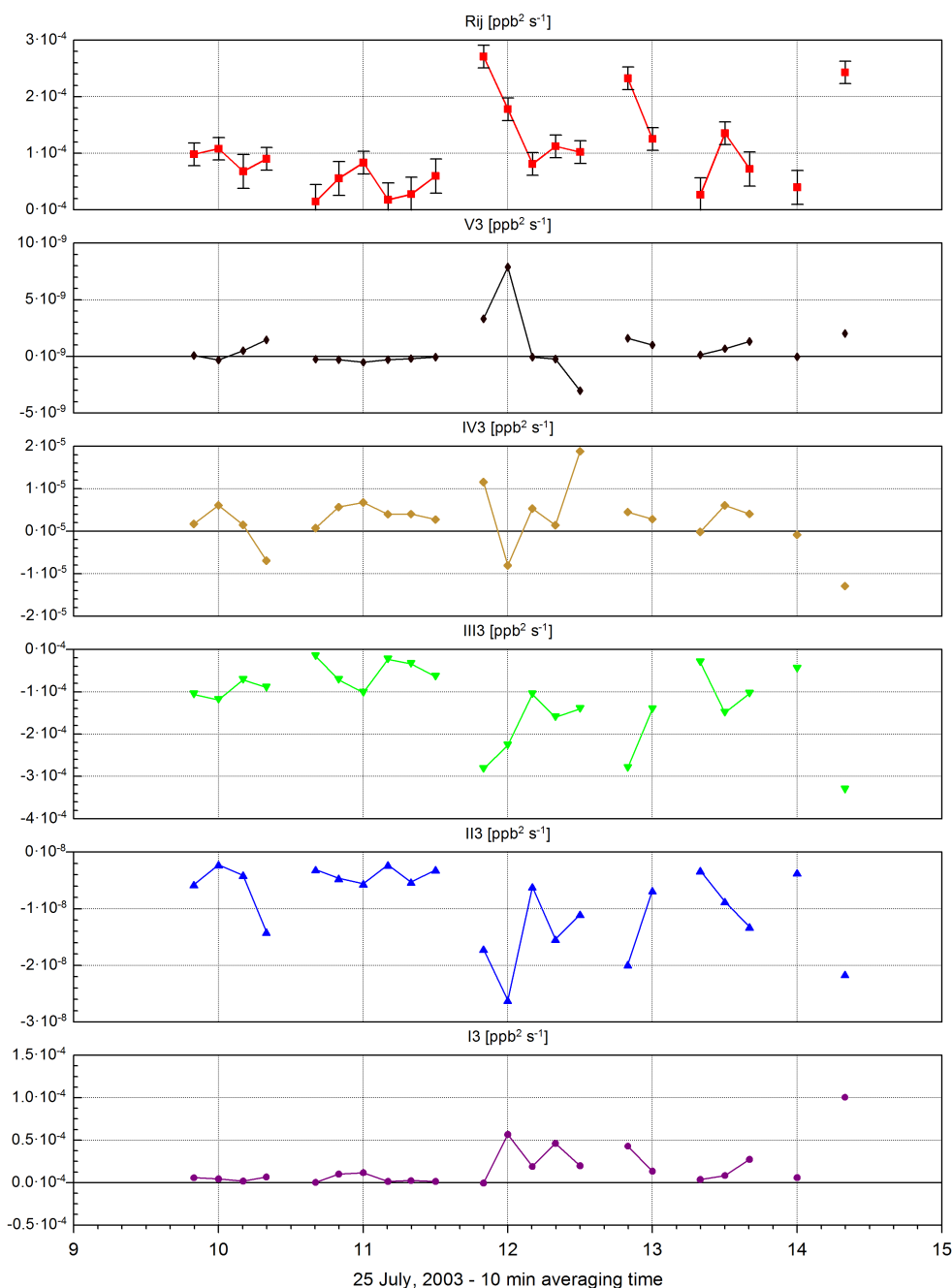
Figure 12. The chemical reaction terms (I3–V3) from Eq. 10 as explained in the text and in Table 4 and the sum R_{ij} of Eq. (10) for day 206 (25 July 2003) of ECHO 2003 at the main tower $z_R = 37$ m.

only the "the chemical reactivity" of the system but also mixing conditions should influence the magnitude of I_S.

4.2.2 Statistical moments

The segregation intensity I_S is composed of the product of normalised standard deviations of isoprene and OH (Fig. 6) multiplied by the correlation coefficient r_{ij} if Eqs. (7) and (8) are combined. Both normalised standard deviations tend to increase with decreasing mixing ratios of isoprene respectively OH_{mod} (but also OH_{mean} itself). For mixing ratios above about 0.8 ppb, a limiting value of $std(ISO)/ISO \approx 0.5$ is observed. For OH all data points are near or above $std(OH)/OH \approx 0.25$. For low mixing ratios $std(ISO)/ISO \approx 1.6$ and $std(OH)/OH \approx 0.45$ are found (Fig. 6). Therefore two limits exist for I_S: for low mixing ratios $r_{ij} \times 1.6 \times 0.45 = 0.72 \times r_{ij}$ and for high mixing ratios
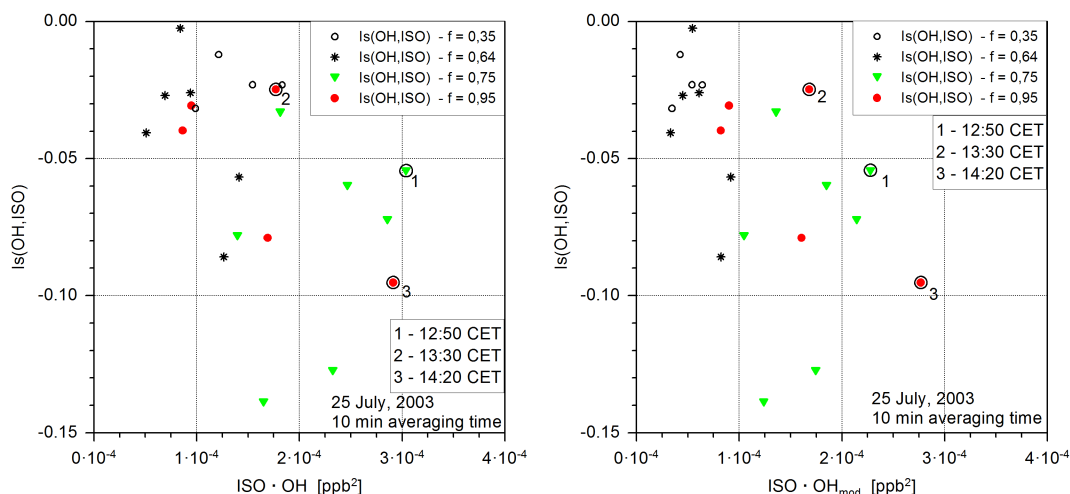
Figure 13. The intensity of segregation as a function of the product of mixing ratios of isoprene and OH and OH_{mod} for different classes of factor f. The three data points 1–3 are explained in Sect. 5.3.2.
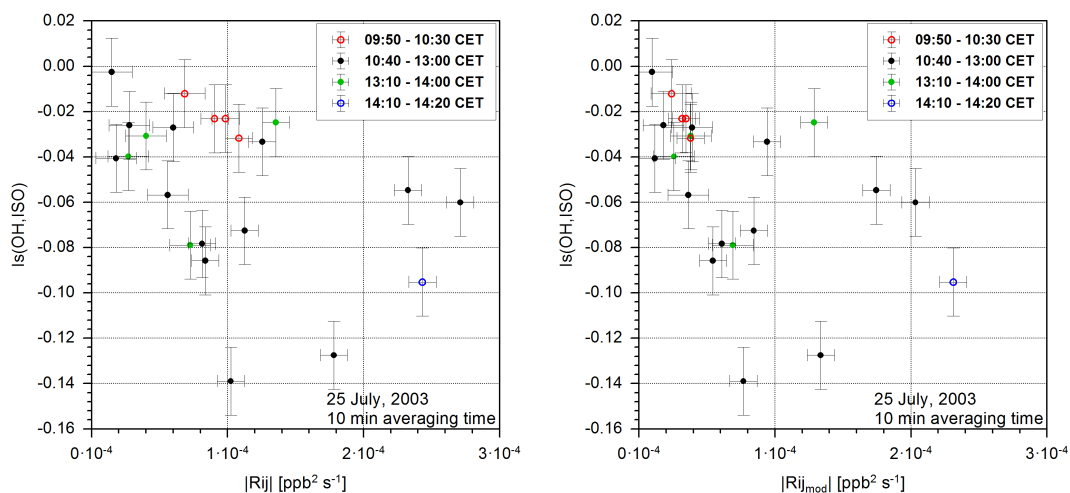

Figure 14. The intensity of segregation as a function of R_{ij} and $R_{ij\,mod}$ with data points indicated for different reaction conditions (see text).

$0.5 \times 0.25 \times r_{ij} \approx 0.125 \times r_{ij}$ can be estimated from data. The correlation coefficient r_{ij} increases with increasing product of mixing ratios $ISO \times OH$ (Fig. 7) and becomes zero for $ISO \times OH = 0$. The comparable behaviour is visible for r_{ij} as a function of $OH_{mod} \times ISO$. But the influence of other reactants changes the slope of the increase of r_{ij} with increasing product of mixing ratios which is proportional to the mean reaction rate for both compounds. In addition not only the chemical state of the atmosphere (here considered by factor f) but also dynamic and mixing conditions influence r_{ij}. This is indicated especially for three periods in Fig. 7 which show a reduced correlation coefficient for otherwise comparable products of mixing ratios. If a mean linear increase of $r_{ij} \approx 3000 \times ISO \times OH_{mod}$ is taken, the correlation coefficients for data points 1–3 would be $r_{ij}(1) \approx -0.675$, $r_{ij}(2) \approx -0.48$ and $r_{ij}(3) \approx -0.82$. The different conditions

which cause a decorrelation between reactants and a reduction of r_{ij} are discussed in Sect. 4.2.5.

4.2.3 Deviation from quasi-linear relationship

In Fig. 4. two data points in the right panel are still above the upper dotted line. The small value $I_S \approx -0.003$ (10:40 CET) is for a situation when a downward advection with mean vertical wind $\overline{w} \simeq -0.25\,\mathrm{m\,s^{-1}}$ transports air from a layer above the forest with isoprene mixing ratios below 0.3 ppb to the measuring site. For this condition the correlation between locally produced OH and advected isoprene decreases ($r_{ij} = -0.02$). Also the product of the normalised standard deviations $\mathrm{std}(ISO)/\overline{ISO} = 0.51$ and $\mathrm{std}(OH)/\overline{OH} = 0.26$ with r_{ij} results in $I_S \approx -0.003$ if Eqs. (7) and (8) are combined. Note that, for all cases during ECHO 2003 with downward-directed $\overline{w}$, the normalised standard deviation of isoprene
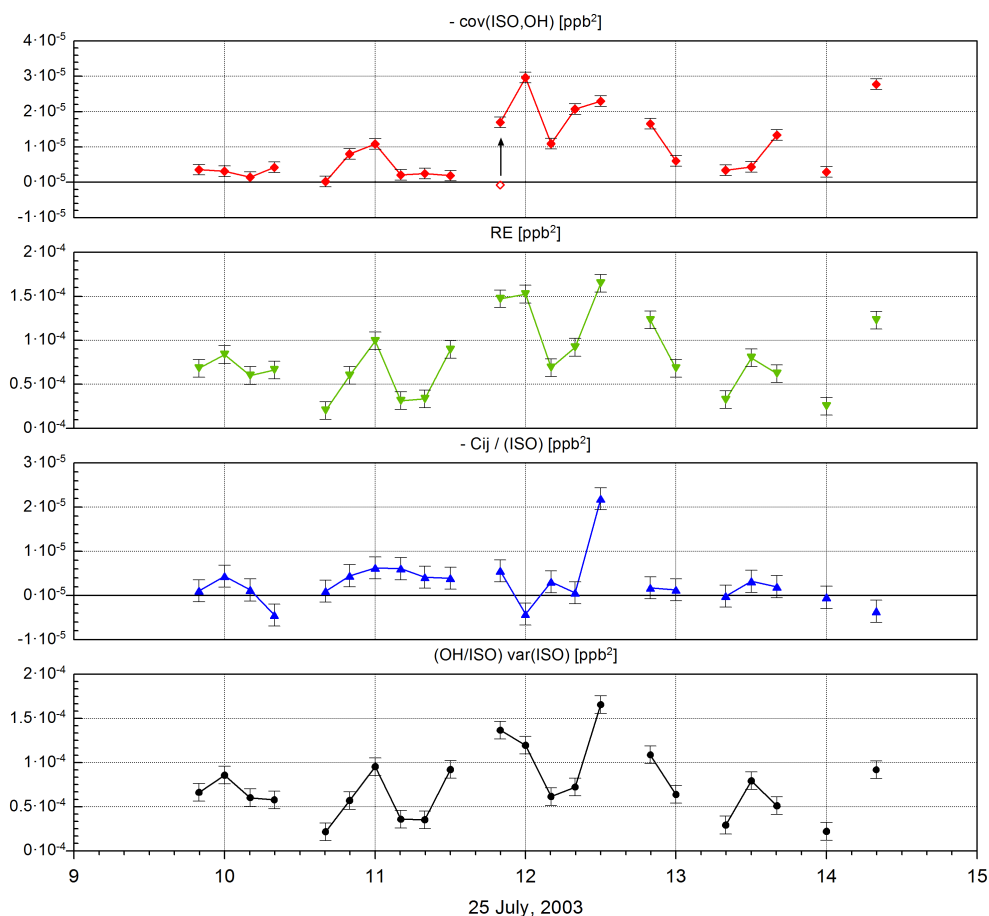
Figure 15. The four terms of Eq. (15) solved for RE as a function of time.

becomes small. A comparable behaviour is observed also for temperature. Also the correlation between isoprene mixing ratio and temperature becomes small for such cases (see Dlugi et al., 2010). It appears that temperature and isoprene are better correlated if a direct influence of the emission source E is detected, because E itself is dependent also on leaf surface temperature and its variance (Ciccioli et al., 1997; Guenther et al., 2006). Therefore, these quantities are less correlated if upward transported isoprene comes down again from atmospheric layers up to some hundred metres above the surface with only smaller temperature variance (e.g. Stull, 1988).

The other point ($I_S = -0.02$, $OH_{mod} = -2.04 \times 10^{-4}$ ppb) at 13:30 CET is for a secondary maximum in $J(O^1D)$, for $\overline{w} \simeq 0\,\mathrm{m\,s^{-1}}$ and upward-directed turbulent fluxes of heat and moisture. The isoprene flux is small and below detection limit for this case. The correction factor $f = 0.95$ is for $\overline{L(OH)} = 4.18\,\mathrm{s^{-1}}$ (Table 2), but has to be reduced only by 20 % for a shift of this data point to the area within the dotted lines (Fig. 4). Even if the variability of NO_2 around the hourly mean value in Table 1 is considered, the lowest possible value is $f = 0.9$ but not $f \leq 0.79$ as required. This

may be caused by a short time maximum in OH production $P(OH)$ by ozone photolysis (and photolysis of other compounds like HONO Kleffmann et al., 2005) occurring around 13:30 CET (Fig. S1 in the Supplement), which is too short to result also in an increase of measured mean $\overline{OH}$ relative to the loss term $\overline{L(OH)}$ being dominated by isoprene reaction in this time interval.

4.2.4 Covariance and mean reaction rates

The segregation intensity I_S is composed of the covariance divided by the product of the means (Eq. 7). But both terms are correlated to a certain extent, because the covariance term increases with increasing product $\overline{c_i} \times \overline{c_j} = [ISO][OH]$ (Fig. 8). This is a qualitative relationship also described by Verver et al. (1997) and Patton et al. (2001) in their model studies.

An upper limit of 3.1×10^{-4} ppb^2 is observed for $\overline{c_i} \times \overline{c_j} = [ISO][OH]$ in Fig. 8 which is also reflected in the data of Fig. 1. The line (a) is given for $I_S = -1$, the case with no reaction between isoprene and OH, while line (b) is for $I_S = 0$, e.g. when the covariance between isoprene and OH is zero. Most data are in the range $-0.1 \leq I_S < 0$ with the diagonal

representing $I_S = -0.1$. For $\overline{c_i} \times \overline{c_j}_{\text{mod}}$ (Fig. 8) the covariance increases nearly linearly as also proposed by the model results. This also agrees with the behaviour of r_{ij} shown in Fig. 7. As a consequence also $-I_S$ increases with increasing product of mixing rations (Fig. 4). The behaviour of both reactants c_i and c_j are influenced by the chemical mixture of the air, the biochemical emission processes from plants and transport and mixing in the canopy flow and the ABL.

As discussed later on, finally the segregation intensity I_S itself increases with increasing product $\overline{c_i} \times \overline{c_j}$ respectively $\overline{c_i} \times \overline{c_j}_{\text{mod}}$ (Fig. 13). Therefore, also $-I_S$ increases proportionally to the mean reaction rate. If the calculation is performed with the measured $c_j = \text{OH}$ mixing ratio, two groups of data points remain in Fig. 7. If the amount of f is considered in $-I_S$ vs. $\overline{c_i} \times \overline{c_j}_{\text{mod}}$, all data points for $f = 0.35$ move to small values. Only three to six values remain outside the left group for $f = 0.75$ and $f = 0.95$. For the marked three points $c_{j\,\text{mod}} = \text{OH}_{\text{mod}}$, the factor f is always about $f = 0.75$ or larger, $\overline{w}$ is slightly positive (14:20 CET) or zero (13:30 CET) and the emissions originate from areas next to the measuring site (Supplement Sect. 3.3.2 with Fig. S20). For 12:50 CET a small negative $\overline{w} < -0.01\,\text{m s}^{-1}$ and a negative isoprene flux is observed (Dlugi et al., 2010).

Therefore, an influence of downward isoprene transport can be assumed for the data point at 12:50 CET. As a consequence, the local production and consumption of OH is less correlated to isoprene ($r_{ij} = -0.27$) than is found for other data points (see Sect. 4.2.5, Fig. 7).

At 13:30 CET not only vertical wind speed diminishes ($w \approx 0$), but also the turbulent flux is below detection limit and therefore called zero.

One possibility to interpret the shift of point 2 "to the right" is that a short-time enhanced production of OH occurs above canopy as discussed above (Sect. 4.2.3, see also Fig. 4).

The chemical and dynamical conditions at 14:20 CET are characterized by a mean updraft ($\overline{w} = 0.2\,\text{m s}^{-1}$) and a relatively high turbulent flux of isoprene ($0.16\,\text{ppb m s}^{-1}$) (Dlugi et al., 2010) with a small footprint of $X \leq 100\,\text{m}$ (see Supplement Fig. S20) and a moderate mixing ratio $c_{j\,\text{mod}} = \text{OH}_{\text{mod}} \approx 1.8 \times 10^{-4}\,\text{ppb}$. Before and after that time interval, the stratification of the atmosphere above canopy was slightly stable (Dlugi et al., 2010).

Summarising these results, the intensity of segregation I_S for the reaction between isoprene and OH reaches maximum values if isoprene becomes the dominant sink for OH. Therefore, for NO_x-rich conditions in the morning (Tables 1 and 2) the loss of OH by NO_2 is important and I_S has minimum values for $f < 0.4$ by the influence of other concurrent reactants. But I_S strongly varies for a fixed value of f (see Fig. 5). This hints towards additional influences of turbulent mixing in the atmospheric flow and emission source strength E (Ciccioli et al., 1997), both acting on $\sigma(\text{ISO})$ and r_{ij} in Eq. 8 as discussed below and in Sect. 6.

4.2.5 Dependence on correlation coefficient and isoprene standard deviation

During situations with OH higher than $(2-3) \times 10^{-4}\,\text{ppb}$ and isoprene above $0.8\,\text{ppb}$, the largest values of I_S are found. The correlation coefficient (see Eq. 8) is in the range $-0.56 \leq r_{\text{ISO OH}} \leq 0$ (Fig. 9), and the normalised standard deviations (Fig. 6) vary in the range $0.38 \leq \sigma(\text{ISO})/\overline{\text{ISO}} \leq 1.5$ and $0.23 \leq \sigma(\text{OH})/\overline{\text{OH}} \leq 0.44$ and $0.25 \leq \sigma(\text{OH}_{\text{mod}})/\overline{\text{OH}_{\text{mod}}} \leq 1.02$ (Fig. 6).

The lowest possible value of the product of normalised standard deviations is 0.09, and therefore any $|I_s| < 0.09$ must be caused by $|r_{ij}| < 1$ (Fig. 9). In addition, for larger segregation intensities $I_S < -0.08$ a limiting range $-0.55 > r_{\text{OH ISO}}$ is calculated. Following the dependence of the covariance (Fig. 8), also the correlation coefficient increases with the increasing product of mean mixing ratios (Fig. 7) or the mean reaction rate. This result differs from those obtained from model calculations (e.g. Vinuesa and Vilà-Guerau de Arellano, 2005; Ouwersloot et al., 2011), with $r_{\text{ISO OH}} > -0.70$ for the comparable magnitude of I_S. Applying these values to the field data, the resulting I_S would be larger up to about a factor of 2 with maxima in the range $-0.3 \leq I_S \leq -0.2$. By a comparable assumption on r_{ij}, Pugh et al. (2011) obtained I_S values larger than determined in our study (Figs. 4, 9).

We will shortly discuss one possibility for such differences. For this analysis the covariance in Eq. (7) may be replaced by Eq. (8) resulting in the product of r_{ij} with normalised standard deviations of isoprene and OH (Fig. 6).

For both compounds the normalised standard deviation, also called the turbulence intensity $\sigma/\overline{c}$, approaches some limiting value for large mixing ratios with about $\sigma_i/\overline{c_i} \approx 0.45$–0.55, if also data of Spirig et al. (2005) are taken into account, and $\sigma_j/\overline{c_j} \approx 0.23 - 0.3$ (Fig. 6) or $\sigma_j/\overline{c_j}_{\text{mod}} \approx 0.25$–0.3.

Extrapolating to small mixing ratios (Fig. 6) yields limiting values of normalised standard deviations for low isoprene mixing ratios of about 1.5, for OH mixing ratios of about 0.45 and for OH_{mod} of about 1.0.

Note that the detection limits ($S/N = 2$) on 25 July 2003 were 41 pptv for isoprene and 0.1 ppt for OH (Dlugi et al., 2010). Therefore all 10-minute mean values given in Fig. 1 are above those limits, but OH_{mod} may be smaller. Not all data points for OH in Fig. 1 are far above this detection limit of the LIF for highly time-resolved measurements.

Uncorrelated noise on the OH time series has no influence on the covariance term, e.g. in Eq. (7), but may have enhanced σ_{OH} in Eq. (8) and $\sigma_{\text{OH}}/\overline{\text{OH}}$, because some data are not very far from detection limit (DL). This differs for isoprene with $\text{DL} = 41\,\text{ppt}$. Therefore, if standard deviations are used to calculate r_{ij}, the corresponding variance of the measured OH, $\sigma_{\text{OH}}^2 = \sigma_{\text{OH}}^2(\text{signal}) + \sigma_{\text{OH}}^2(\text{noise})$, and so $\sigma_{\text{OH}}(\text{signal})$, may be too high. If a large contribution of noise $\sigma_{\text{OH}}^2(\text{signal})/\sigma_{\text{OH}}^2(\text{noise}) = 2$ is assumed, σ_{OH} is a factor of

1.23 too large. With mean values of $\sigma_{\mathrm{ISO}}/\overline{\mathrm{ISO}} = 0.65$ and $\sigma_{\mathrm{OH}}/\overline{OH} = 0.3$ and with a corrected term $\frac{1}{1.23} \times \frac{\sigma_{\mathrm{OH}}}{\mathrm{OH}}$ (Fig. 6), the derived correlation coefficient would be larger by about the same factor of 1.23, and the maxima would be shifted to r_{ij}(corrected) ≈ -0.67. But even r_{ij}(corrected) is still below the assumption made for model calculations.

Note that a correlation coefficient $|r_{ij}| < 1$ also describes the deviation of the probability distributions of c_i and c_j from a normal distribution type (see Dlugi et al., 2010). Therefore the distributions of the mixing ratios of isoprene and OH during this field study differ from the normal distribution as often assumed or computed in model studies (e.g. Vinuesa and Vilà-Guerau de Arellano, 2005; Ouwersloot et al., 2011).

Combining the results from the ECHO field study, a relation between I_{S} and the standard deviation σ_i of isoprene is found (Fig. 10) (here again the data point $I_{\mathrm{S}} \simeq 0$, $\sigma_i = 0.67$ ppb is shifted to $I_{\mathrm{S}} = -0.06$ and $\sigma_i = 0.67$ ppb as discussed in Sect. 5.3.4). Another point ($I_{\mathrm{S}} = -0.002$; $\sigma_i = 0.18$) is for a small covariance of -2×10^{-7} ppb^2 but agrees with an increase of I_{S} with increasing σ_i. Note that this data point is for the conditions at 10:40 CET with a significant vertical advection (Sect. 4.2.3). Therefore, for the same range of σ_i the intensity of segregation I_{S} varies by a factor of about 4 in the data set. $|I_{\mathrm{S}}|$ increases with increasing $\sigma(i)$, but two branches are obtained with different proportionality between both quantities. This behaviour changes if I_{S} is presented as a function of normalised variance of isoprene nvar(ISO) = nvar(c_i) on the right side of Fig. 10 with the exception of two data points at 10:00 CET and 11:30 CET. For those points nvar(ISO) is large while r_{ij} and nvar(OH) are small. Therefore also $I_{\mathrm{S}} = r_{ij}(\sigma_i/\overline{c_i})(\sigma_j/\overline{c_j})$ respectively $I_{\mathrm{S}} = r_{ij}(\sigma_i/\overline{c_i})(\sigma_j/\overline{c_j}_{\mathrm{mod}})$ becomes significantly smaller than for other conditions of comparable nvar(ISO).

In Sects. 5.3 and 6 we further discuss the relevance of σ_i and normalised variances for the behaviour of I_{S} as an influence of chemical reactions on the balance of covariance between isoprene and OH. Although further reactions have influenced the OH budget in our case (see Sect. 2.3) and transport and mixing conditions change during the 6 h of the experiment on 25 July 2003 (day 206), the general behaviour of the absolute value of I_{S} – an increase with increasing σ_i in Fig. 10 – remains.

The error bars in Fig. 10 are given by the uncertainty of the covariance between isoprene and OH if the time delay between both time series is varied by up to ± 0.2 s. This is due to the fact that the wind vector varies inside the sampling volume of separated gas inlets and the METEK anemometer (Dlugi et al., 2010) during each 10 min interval. The "high-frequency loss" of covariance as discussed by Spirig et al. (2005) is not added because the spectral behaviour of both time series is not known above 0.2 Hz.

The number of time intervals (10 min averages) and so the number of derived values in our case study is limited, since the experimental setup was operated only some hours in the mode presented here. Therefore, in the following, the balance

equation for the covariance between isoprene and OH will be discussed and applied as a tool for the further analysis of field data to finally evaluate the relative and absolute influences of chemical reactions, turbulent and convective mixing and advection on the magnitude of the segregation intensity I_{S}.

5 Balance equations for the covariance between isoprene and OH and the segregation intensity I_{S}

5.1 The equations

The balance equation for the covariance of two reacting compounds (Eq. 9) was used by Verver et al. (2000) and Patton et al. (2001) obviously in a simplified version (a) neglecting advective terms (A) and (b) neglecting horizontal turbulent diffusion.

The analysis of the data from the experiment ECHO 2003 allows for some hours of day 206 (09:00–15:00 CET) to calculate a number of terms of Eq. (9), and to estimate their possible maximum and minimum contributions to the balance of $\overline{c_i' c_j'}$ for the isoprene concentration c_i and the OH concentration c_j.

In the complete form the balance equation for $\overline{c_i' c_j'}$ reads as follows (e.g. Sorbjan, 1989; Stull, 1988; Schumann, 1989; Verver et al., 1997):

$$
\underbrace{\frac{\partial}{\partial t} \overline{c_i' c_j'}}_{S} = \underbrace{-\overline{u_k' c_i'} \frac{\partial \overline{c_j}}{\partial x_k}}_{\mathrm{TPI}_k} \underbrace{-\overline{u_k' c_j'} \frac{\partial \overline{c_i}}{\partial x_k}}_{\mathrm{TPOH}_k} \underbrace{-\overline{c_i' c_j'} \frac{\partial \overline{u_k}}{\partial x_k}}_{A_{1k}} \underbrace{-\overline{u_k} \frac{\partial}{\partial x_k} \overline{c_i' c_j'}}_{A_{2k}} \underbrace{-\frac{\partial}{\partial x_k} \overline{u_k' c_i' c_j'}}_{\mathrm{TT}_k}
$$
$$
\underbrace{-(\nu_i + \nu_j) \left(\frac{\partial c_i'}{\partial x_k} \right) \left(\frac{\partial c_j'}{\partial x_k} \right)}_{D} + \underbrace{R_{ij}}_{R_{ij}}, \tag{9}
$$

where index $k = 1$ (coordinate x and wind coordinate u); $k = 2$ for y and v; $k = 3$ for z and w, and S is the storage term; TPI_k is the turbulent production by a turbulent flux of isoprene in a spatially inhomogeneous field of OH; TPOH_k is turbulent production by a turbulent flux of OH in a spatially inhomogeneous field of isoprene; A_{1k} is advection of covariance by the influence of the divergence of the flow field; A_{2k} is the advection of covariance with the mean flow; TT_k is the turbulent transport of covariance; D is molecular diffusion term; and R_{ij} is the chemical reaction term.

The chemical reaction term (Eq. 10) is formulated according to Donaldson and Hilst (1972), Vilà-Guerau de Arellano et al. (1995) and Vilà-Guerau de Arellano and Lelieveld (1998) for atmospheric conditions and was also applied by Verver et al. (1997, 2000) and Patton et al. (2001) for a bimolecular reaction in the following form with the abbreviations I3 to V3 (from the left to the right, third order) for the five third-order terms in brackets (see Table 4):

$$
R_{ij} = -k_{ij} \left[(\overline{c_i' c_j'})(\overline{c_i} + \overline{c_j}) + \overline{c_i}\, \overline{c_j'^2} + \overline{c_j}\, \overline{c_i'^2} \right.
$$
$$
\left. + \overline{c_i' c_i' c_j'} + \overline{c_i' c_j' c_j'} \right]. \tag{10}
$$

The data analysis in Sect. 5.3 (Figs. 11, 12) with Eq. (9) proves that the data set of the ECHO 2003 study fulfills the criteria of stationarity. For these conditions Eq. (9) may be simplified:

$$S \equiv 0 = -\mathrm{TPI}_k - \mathrm{TPOH}_k - A_{1k} - A_{2k}$$
$$- \mathrm{TT}_k - D + R_{ij}. \tag{11}$$

This allows us to find a new expression for $\overline{c_i' c_j'}$ in terms of all other quantities in Eq. (11) because this covariance also explicitly appears in the first term of R_{ij} (Eq. 10). The resulting diagnostic equation (Eq. 12) reads

$$\overline{c_i' c_j'} = -\frac{1}{k_{ij}(\overline{c_i} + \overline{c_j})} \Big[(\mathrm{TPI}_k + \mathrm{TPOH}_k + A_{1k} + A_{2k} + \mathrm{TT}_k + D) \\ -k_{ij} \Big(\overline{c_i}\, \overline{c_j'^2} + \overline{c_j}\, \overline{c_i'^2} + \overline{c_i' c_i' c_j'} + \overline{c_i' c_j' c_j'} \Big) \Big]. \tag{12}$$

In Sect. 5.2 we simplify Eq. (12) applying also some order of magnitude estimations for some terms. The fast measurements of fluctuations of mixing ratios of isoprene and OH in a small volume of air on 25 July 2003 were performed only at one point (7 m above canopy height, $h_c = 30$ m) at the ECHO main tower (Sect. 2 and Supplement 3.2; see also Dlugi et al., 2010). Spatial derivations of mixing ratios of these compounds and their fluxes are not available from this data set but from other measurements (Supplement Sect. 3). Therefore, to estimate the contribution by all terms which describe turbulent production and transport as well as advection, we may summarise these effects in a residual term (RES) – in the mathematical sense – as

$$\mathrm{RES} = \mathrm{TPI}_K + \mathrm{TPOH}_k + A_{1k} + A_{2k} + \mathrm{TT}_k + D. \tag{13}$$

This enables us to estimate the resulting influences of these processes on the covariance and I_S, although these detailed complex measurements were done only at one measuring height $z_R = 37$ m (Supplement Sect. 2).

Also the chemistry term in Eq. (12) may be written in the following manner to separate the term with the variance of isoprene which shows a direct relation to I_S (Fig. 10) (e.g. Patton et al., 2001; Verver et al., 1997) from all other terms C_{ij}:

$$R_{ij,\mathrm{res}} = -k_{ij}(\overline{c_j}\,\overline{c_i'^2} + C_{ij}). \tag{14}$$

Here C_{ij} is the sum of terms two (II3), four (IV3) and five (V3) on the right side of Eq. (10).

For isoprene (i) and OH (j) with $\overline{c_i} \gg \overline{c_j}$ (e.g. Dlugi et al., 2010), the prefactor in Eq. (12) can be simplified, and, therefore, Eq. (12) finally reads

$$-\overline{c_i' c_j'} = \frac{1}{k_{ij}\overline{c_i}}(\mathrm{RES}) + \frac{k_{ij}}{\overline{c_i}\,k_{ij}} C_{ij} - \frac{\overline{c_j}}{\overline{c_i}}\overline{c_i'^2} \\ = \frac{1}{k_{ij}\overline{c_i}} \big[\mathrm{RES} + k_{ij} C_{ij} \big] - \frac{\overline{c_j}}{\overline{c_i}}\overline{c_i'^2} \tag{15} \\ = \mathrm{RE} + \frac{C_{ij}}{\overline{c_i}} - \frac{\overline{c_j}}{\overline{c_i}}\overline{c_i'^2}.$$

Table 3. Order of magnitude of terms of the balance equation of the covariance (Eq. 9) in ppb^2 s^{-1} as explained in Sects. 5.2 and 5.3 for $x_k = z$ (vertical coordinate) and the mean error estimate.

Term	Range [ppb^2 s^{-1}]	Mean error [%]
S	$< 6 \times 10^{-8}$	± 30
TPI_k	6×10^{-7} to 6×10^{-6}	± 43
TPOH_k	6×10^{-7} to 6×10^{-6}	± 48
A_{1k}	$< 10^{-6}$	± 36
A_{2k}	$\leq 8 \times 10^{-7}$ ($< 4 \times 10^{-4}$)	± 80 (± 30)
TT_k	$< 4 \times 10^{-6}$	± 60
D	$< 10^{-10}$	± 60
R_{ij}	$< 4 \times 10^{-4}$	± 16

Therefore, for the reaction of isoprene with OH the covariance controlling the segregation intensity (Fig. 8) is determined by the product between the quotient of the mixing ratios of OH (c_j) and isoprene (c_i) times the variance of isoprene and two other terms. These terms describe the interactions of turbulent mixing and chemistry (RES) (see Eq. 13) and mainly third-order chemical correlation terms (C_{ij}) in the turbulent fields of reactants.

Dividing Eq. (15) by the product of the means, a new diagnostic equation Eq. (16) for I_S (see Eq. 7) can be formulated.

$$-I_S = -\frac{\overline{c_i' c_j'}}{\overline{c_i} \times \overline{c_j}} \\ = \frac{\mathrm{RES}}{k_{ij} \times \overline{c_i} \times (\overline{c_i} \times \overline{c_j})} + \frac{C_{ij}}{\overline{c_i}(\overline{c_i} \times \overline{c_j})} - \frac{\overline{c_i'^2}}{\overline{c_i}^2} \tag{16} \\ = \mathrm{RE}_{is} + \mathrm{CH}_{is} - \mathrm{nvar}(\mathrm{ISO})_{is}$$

The third term $\mathrm{nvar}(\mathrm{ISO})_{is}$ of Eq. (16) is the normalised variance (one term in R_{ij_res}) with some proportionality vs. σ_{ISO} itself and I_S (Fig. 10). The second term CH_{is} summarises all other terms from from R_{ij_res} in C_{ij}. It becomes also important by the inverse influence of $\overline{c_j} < 10^{-3}$ ppb. The first term RE_{is} is again determined as a residuum, as all other terms of Eq. (16) are directly calculated from measurements at height $z_R = 37$ m at the ECHO main tower (Sect. 3 and Supplement Sect. S2).

5.2 The terms of the balance equation of the covariance

In the following all terms of the balance equation Eq. (9) are estimated by their order of magnitude based on measured data from the field study ECHO 2003 (Supplement Sects. S2 and S3) and calculated quantities like first to fourth moments (Ammann et al., 2004; Dlugi et al., 2010; Kleffmann et al., 2005; Schaub, 2007; Spirig et al., 2005). This also helps to specify the impact of different processes on the residual terms RES, RE or RE_{is}. Terms which cannot be determined this way, because the highly time-resolved measurements were performed only at one measuring point, are estimated based on additional data from the ECHO field study

Table 4. Order of magnitude (amount) of the five third-order terms (I3)–(V3) (as indicated by number 3) of R_{ij} [ppb^2 s^{-1}] (Eq. 10) according to the analysis in Sect. 5.3 (see also Fig. 12).

	Term	Third moment	Range [ppb^2 s^{-1}]
I3	R_{ij_1}	$k_{ij}\left[\overline{(c_i'c_j')}(\overline{c_i}+\overline{c_j})\right]$	7×10^{-6} to 1.3×10^{-4}
II3	R_{ij_2}	$k_{ij}\left[\overline{c_i}\,\overline{c_j'^2}\right]$	10^{-7} to 10^{-8}
III3	R_{ij_3}	$k_{ij}\left[\overline{c_j}\,\overline{c_i'^2}\right]$	$\simeq 10^{-4}$
IV3	R_{ij_4}	$k_{ij}\left[\overline{c_i'c_i'c_j'}\right]$	$< 3\times10^{-5}$
V3	R_{ij_5}	$k_{ij}\left[\overline{c_i'c_j'c_j'}\right]$	$< 10^{-8}$

(Ammann et al., 2004; Bohn, 2006; Bohn et al., 2006; Kleffmann et al., 2005; Schaub, 2007; Spirig et al., 2005).

If advection with the mean flow is neglected and only the residual transport in the vertical direction is considered, Eq. (9) is simplified and is consistent with the equations as applied by Verver et al. (1997) and Patton et al. (2001) for their model studies, while Eq. (10) is identical to their formulations.

For the following estimation of the order of magnitude of all terms of Eq. (9), A_{1k} and A_{2k} are not neglected, but for some terms only changes in z direction are considered which simplifies the first and second term on the right side of Eq. (9). The storage term (Fig. 11) is always smaller than most other terms (Table 3) and can be neglected to formulate diagnostic equations for the covariance and I_S (Sect. 5.1). The first term of RES on the right side is the product of the turbulent isoprene flux and the mean vertical gradient of OH mixing ratio, which can be estimated from measurements during ECHO 2003 (Dlugi et al. (2010), Supplement Sects. 2 and 4). The isoprene flux varies in the range 0.02–0.2 ppb m s^{-1} (see Dlugi et al., 2010; Spirig et al., 2005), and the mean gradient of OH above canopy – from unpublished measurements – is about 3×10^{-5} ppb m^{-1}. Thus the combined first term is 6×10^{-7} to 6×10^{-6} ppb^2 s^{-1} (Table 3). The second term is obtained if isoprene and OH are replaced. The vertical gradient of isoprene (see Schaub, 2007; Ammann et al., 2004) varies in the range ±0.14 ppb m^{-1} to ±0.01 ppb m^{-1} and the OH flux between zero and -4×10^{-5} ppb m s^{-1} (Dlugi et al., 2010). Note that the vertical turbulent flux of OH is caused by transport of compounds like isoprene and others (e.g. Table 1) to the measuring volume where they locally react with OH. The product is of the same order of magnitude as the first term TPI$_k$. Depending on the sign of TPI$_k$ and TPOH$_k$, in an order of magnitude estimation, both terms may cancel out each other or may add up to about 1.2×10^{-5} ppb^2 s^{-1} (Table 3).

In the balance equation of the covariance between isoprene and OH, the advection term is decomposed into terms A_{1k} and A_{2k}. On a local scale the divergence of the wind field in A_{1k} – especially under the influence of tall vegetation and complex terrain (e.g. Sun, 2007; Stull, 1988) – can be as large as 0.1s^{-1} but may decrease to $10^{-3}-10^{-2}\text{s}^{-1}$ for small mesoscale circulation (e.g. Stull, 1988). With the covariance in the range of 10^{-5} ppb^2 (Fig. 8), term A_{1k} becomes smaller than 10^{-6} ppb^2 s^{-1} (Table 3).

The term A_{1k} is not added to the covariance on the left side of Eq. (12) because in general the wind field divergence is $< 0.1\text{s}^{-1}$, and, therefore, the covariance on the left side of Eq. (12) will only be influenced by less than 10 %.

The other term A_{2k} is estimated to be below 8×10^{-7} ppb^2 s^{-1} if the spatial gradient of the covariance is proportional to the change of the standard deviation of isoprene σ_i with time. This relation is empirically derived from measurements at the main and the west tower. But the discussion in Sect. 5.3.3 shows that this approximation may be not valid on our day 206.

The spatial variability of $\overline{c_i'c_j'}$ is caused by local variability of OH mixing ratio caused by photolysis and chemical reactions during advection of isoprene from emission sources to the site of measurements. As discussed in Sect. 5.3.4, OH production and isoprene emission are found to be locally positively correlated in a frequency range below about 0.02 Hz.

The covariance for inhomogeneous mixing conditions describes a negative correlation between isoprene and OH (Fig. 8). Therefore, as mostly negative covariances are determined, the change from locally positive to negative correlation is caused by advective transport of isoprene and isoprene variance through the field of OH being variable in time and space. The influence of advection on this term possibly can be significantly larger as discussed below and shown in Table 3 in parentheses. The influence of horizontal derivations in A_{2k} is discussed further below and in Sects. 5.3.3, 6.2 and in Sect. S4 in the Supplement.

Compared to other terms which compose RES or RE$_{is}$ (Eq. 16), A_{1k} can be neglected if the divergence of the wind field is below 10^{-1}s^{-1}.

The term TT$_k$ is given by the divergence of the turbulent transport of the numerator of segregation intensity. The turbulent transport is also one term in the chemical part of the flux balance (e.g. Patton et al., 2001) and is calculated directly from measured quantities at $z_R = 37$ m. This term is generally below $\pm10^{-5}$ ppb m s^{-1} with one exception around 12:00 CET with a value of 3.7×10^{-5} ppb m s^{-1}. The vertical divergence of third-order moments (e.g. of $\overline{w'\theta'q'}$) is found from measurements at the main tower to be at least smaller by an order of magnitude than the moment itself, e.g. smaller than 4×10^{-6} ppb^2 s^{-1} (Table 3). Here the analogy between $q, c_j = $ OH, T and c_i is used as discussed in the Supplement Sect. 4. Therefore, also this term may be of the same order of magnitude as the terms TPI$_k$ and TPOH$_k$.

The molecular diffusion term D is composed of the product of vertical gradients of fluctuations of isoprene (about 10^{-2} ppb m^{-1}) and OH (about 10^{-5} ppb m^{-1}) times the sum

of the molecular kinematic diffusivities of the order of $10^{-5}\,\mathrm{m^2\,s^{-1}}$ based on the data presented by Dlugi et al. (2010). Therefore this term D is smaller than $10^{-10}\,\mathrm{ppb^2\,s^{-1}}$ and can be neglected in the following. (For further discussion see Supplement Sect. 4.)

In this order of magnitude estimation, the maximum of the terms which compose RES is about $1.6 \times 10^{-5}\,\mathrm{ppb^2\,s^{-1}}$ while R_{ij} is below $4 \times 10^{-4}\,\mathrm{ppb^2\,s^{-1}}$ (Table 3), and RES $\simeq R_{ij}$ (Eq. 11) is not fulfilled. Therefore, not only the vertical but also the horizontal derivatives should significantly contribute to all terms without D in Eq. (9). Based on the available data the horizontal contributions to TPI_k and TPOH_k may be estimated to be as large as the vertical contributions. The covariance $\overline{c_i' c_j'} = r_{ij} \times \sigma_i \times \sigma_j$ is always determined locally by the transport of isoprene variance – standard deviation σ_i – through a field of locally variable OH mixing ratio (c_j) characterized by σ_j^2 (Eq. 12). Depending on r_{ij}, the horizontal contributions in A_{2k} may therefore also approach values in the range of 5–$10 \times 10^{-5}\,\mathrm{ppb^2\,s^{-1}}$ and, therefore, significantly contribute to RES, so that the sum approaches the magnitude of R_{ij}.

The chemical reaction rate R_{ij} (Eq. 10) consists of five terms which can directly be estimated from results given by Dlugi et al. (2010) and is discussed in more detail in Sect. 5.3.2 (e.g. Fig. 12, Table 4). The third term $-k_{ij} \times \overline{c_j}\,\overline{c_i'^2}$ (term III3 in Fig. 12) is proportional to the variance of the isoprene mixing ratio and becomes dominant for most 10 min intervals sometimes together with the first term $-k_{ij} \times \overline{c_i' c_j'} (\overline{c_i} + \overline{c_j})$, which should be positive (see term I3 in Fig. 12) by the influence of the covariance, which itself has only negative values. The terms II3 and V3 are small and may be neglected. The magnitude of term IV3 is of the order of term $I3$ but with positive as well as negative values. This points towards the results obtained in Sect. 4.2.5 that the standard deviation (Fig. 10) of isoprene mixing ratio – or normalised variance as in Eq. (16) – controls segregation intensity I_S if isoprene is the dominant hydrocarbon in the gas mixture with respect to the reaction with OH. Therefore, as discussed in Sect. 4.2.1, an extended analysis is necessary because concurrent reactants like CO, NO_2 and NO with mixing ratios higher by a factor of 2 or 4 in the morning hours (09:00–10:40, 11:10–11:30 CET) than during other time intervals of day 206 (25 July 2003) are observed (Table 1). (See also Supplement Sect. S3.) This aspect and its influence on R_{ij} is further discussed in Sect. 5.3.

5.3 Results for the balances of covariance and segregation intensity

5.3.1 The storage term

As mentioned before the storage term in Eq. (9) is small and can be neglected compared to other terms (Fig. 11) because of its magnitude of $\pm 10^{-8}\,\mathrm{ppb^2\,s^{-1}}$. This empirical behaviour allows us to simplify Eq. (9) and to derive Eq. (11), the diagnostic form Eq. (12), and, finally, Eq. (15) and Eq. (16) for conditions of 25 July 2003 during ECHO. But this may not reflect the general behaviour of the chemical system at other field sites. For completeness, the storage term of the balance of isoprene mixing ratio is shown, which – in general – is not small compared to other terms as discussed in Sect. 3.

5.3.2 The chemical reaction term

The empirical analysis on the relation between the product of the mixing ratios and the covariance between isoprene and OH (Fig. 8) suggests that the variations of $\overline{c_i' c_j'}$ and I_S (Fig. 13) are better described by the normalised variance of isoprene $\sigma_i^2 / \overline{c_i}^2$ as given on the right side of Fig. 10 than on the isoprene standard deviation σ_i.

This behaviour is also reflected by the third term $\mathrm{nvar}(\mathrm{ISO})_{is} = \overline{c_i'^2}/\overline{c_i}^2$ on the right side of the diagnostic equation for I_S Eq. (16) and, therefore, is consistent with the theoretical concept, which is applied to the data analysis (see Sect. 5.1).

The numerical results for R_{ij} (Eq. 10) support the estimation in Sect. 5.2 (Table 4) but show more details (Fig. 12). All terms in brackets (I3–V3) are third order by dimensions and are given from left (below) to right (fifth term, V3) like in Eq. 10 and Table 4 with the sum of all terms R_{ij} at the top. Term III3 is proportional to the variance of isoprene mixing ratio and, therefore, is dominant while term I3 is negative by the influence of the covariance but changes sign like term III3, because all terms in R_{ij} are multiplied by -1 in Eq. (10). In general I3 has a tendency to reduce the influence of term III3 on R_{ij}. The chemical reaction term R_{ij} enters into Eq. (12) with a negative sign to compensate for positive contributions from terms in RES (see also Eq. 13).

Comparing the storage terms from the balance equations with I_S (Fig. 11) shows that many features of I_S can also be seen in the storage term of the balance for the covariance (Eq. 15) between isoprene and OH and even in R_{ij} and term III3 until about 12:30 CET (Fig. 12).

This dominant term III3 is composed of the quotient $\overline{\mathrm{OH}}/(\overline{\mathrm{Iso}} + \overline{\mathrm{OH}}) \simeq \overline{\mathrm{OH}}/\overline{\mathrm{ISO}}$ and the variance of isoprene, and, therefore, this influence can also be seen in a comparison of I_S to R_{ij} respectively $R_{ij_{\mathrm{mod}}}$ (Fig. 14). Two branches appear in the left part of this Fig. 14 with a different dependence of I_S on R_{ij}. This behaviour is comparable to the dependence of I_S on standard deviation as shown in Fig. 10.

The error for R_{ij} is mainly caused by the uncertainty in the covariance in term I3 and the triple moment in term IV3 when the same calculation as for I_S (e.g. for the covariance) is performed. The accuracy of R_{ij} is mainly caused by the mean error of only 7 % for the normalised variances of isoprene. Although CH_{is} has a maximum error of 64 %, this term contributes only less than 15 % to I_S. Therefore, the resulting errors on I_S are significantly smaller (see Supplement

Sect. S4.1), and the same possible source of uncertainty influences both quantities in the same way.

If only the relative loss of OH caused by isoprene is considered, all terms in R_{ij} become smaller by the correction f described in Sect. 4.2.1 (Table 2) and in Sect. 2.3. Note that all terms in R_{ij} are affected by this procedure if the mixing ration of OH is replaced by $OH_{mod} = f \times OH$, but I_S remains unchanged.

The modification is the largest for the first and second period (Table 2) and almost negligible for the last period. But some data points are still outside the new relation between I_S and $R_{ij_{mod}}$ on the right side of Fig. 14. After 14:00 CET the influence of the maximum value of isoprene mixing ratio and isoprene variance cause maxima in both terms I3 and III3. Therefore also $R_{ij_{mod}}$ has a maximum significantly different from the expected range of the relation to $-I_S$ if smaller and larger values of $|I_S|$ are considered. At least four other data points at 11:50 CET ($I_S = -0.06$), 12:50 CET ($I_S = -0.055$), 13:30 CET ($I_S = -0.024$) and 14:10 ($I_S = -0.095$) with different factors f (Table 2) are shifted still to the right only by the influence of term III3. The variance of isoprene is in the range $0.3 < \sigma_i^2 < 0.46$, and the mixing ratio of $\overline{OH_{mod}}$ is still above 2×10^{-4} ppb. Therefore, their product multiplied by $k_{ij} = 2.3$ ppb^{-1} s^{-1} is larger than for other data points with comparable I_S, but lower OH and OH_{mod} (Fig. 14). We discussed these data points within the context of the relations between the covariance and correlation coefficient on mean reaction rates (Sects. 4.2.2, 4.2.4, Fig. 7). The deviation of f from the mean $\overline{f}$ for each time interval is most likely (Tables 1, 2). In addition, at 12:50 CET, $I_S = -0.055$ is for a situation with a dominating downdraft instead a convective updraft also with a negative net isoprene flux (see Dlugi et al., 2010). The magnitude of $I_S = -0.06$ (at 11:50 CET) is a result of a combined influence of a change in OH production $P(OH)$ and isoprene emission source as discussed in Sect. 5.3.4. The third data point at 13:30 CET is from the period when stable conditions developed above canopy (Dlugi et al., 2010). Therefore these conditions are different compared to all other time intervals with more "common conditions" like (a) an upward-directed isoprene flux, (b) nearly constant relation $P(OH)/L(OH)$ and (c) unstable or neutral stratification above canopy during daytime.

In general, both parameters, σ_i^2 and $\overline{c_j}$ respectively $\overline{c_{j_{mod}}}$ influence R_{ij} ($R_{ij_{mod}}$) during unstable stratification above canopy. At 14:10 CET, like at 14:20 CET for r_{ij} (Fig. 7), R_{ij} ($R_{ij_{mod}}$) is mainly determined by the large variance of isoprene $\sigma_i^2 = 0.78$ ppb^2 during a short interval with unstable stratification and a sensible heat flux $H \simeq 0.1$ K m s^{-1} within a period with otherwise slightly stable conditions after 13:20 CET. Assuming f, and therefore $c_{j_{mod}}$, would be too large, the required reduction in $R_{ij_{mod}}$ is about 50 % at 11:50 CET, 40 % at 12:50 CET and again 50 % at 13:00 CET, 13:30 CET and 14:10 CET.

In addition, all other data points for the relation between $-I_S$ and $R_{ij_{mod}}$ are influenced by the relative contribution of isoprene to the reaction with OH (Tables 1, 2) as well as the change of stratification above canopy which is unstable until 13:20 CET (Dlugi et al., 2010).

Therefore, although isoprene becomes more dominant in OH removal after 13:00 CET the changing mixing conditions on a shorter timescale tend to reduce this influence on I_S. This aspect of influences of turbulence and convection on mixing processes and segregation is further discussed in Sect. 6. In the periods when the atmosphere above canopy becomes partly stable, maximum values of I_S are in between $I_S = -0.07$ (13:40 CET) and $I_S = -0.095$ (14:20 CET), although isoprene is the dominant sink for OH (Tables 1, 2).

This hints again towards a combined influence of chemical reactions (R_{ij}) and turbulent respectively convective mixing and advection (RES, RE$_{is}$) as given in Eqs. (15) and (16).

5.3.3 Covariance and segregation intensity

The covariance $\overline{c_i' c_j'}$ and I_S are influenced by chemical reactions because they can be presented as a function of the mean reaction rate as well as transport and mixing processes (Figs. 8, 13). The latter can only be determined as a mathematical residuum as RE in Eq. (15) or RE$_{is}$ in Eq. (16).

Solving Eq. (15) for RE yields the results in Fig. 15. Note that the covariance itself is negative, so the result becomes positive by the minus sign in Eq. (15). This term is determined from measured data of the order of 10^{-5} ppb^2. Also $-C_{ij}/\overline{c_i}$ and $(\overline{c_j}/\overline{c_i}) \times \sigma_i^2$ are determined from measured data. The latter term is larger by an order of magnitude than both other terms. Therefore RE is largely compensated by $(\overline{c_j}/\overline{c_i}) \times \sigma_i^2$ because the storage term S in Eq. (9) (Fig. 11) is negligible. A comparable result is obtained if Eq.16 is solved for RE$_{is}$ with RE$_{is} \simeq (\sigma_i^2/\overline{c_i^2})_{is}$ (Fig. 16) because the normalisation does not change the relative magnitudes of the different terms. CH$_{is}$ is dominated by the fourth term in Eq. (10) and is only about 15 % or less of the magnitude of $(\sigma_i^2/\overline{c_i^2})_{is}$ Therefore the covariance and I_S are controlled by the difference of two terms being larger by about one order of magnitude than the two other terms (Figs. 15, 16). The magnitudes of RE and RE$_{is}$ support the conclusion in Sect. 5.2 (Table 3) that the magnitude of horizontal derivatives in term A_{2k} should be of the same order as R_{ij} to fulfill the findings $S \simeq 0$ and $R_{ij} \approx$ RES in Sect. 5.1.
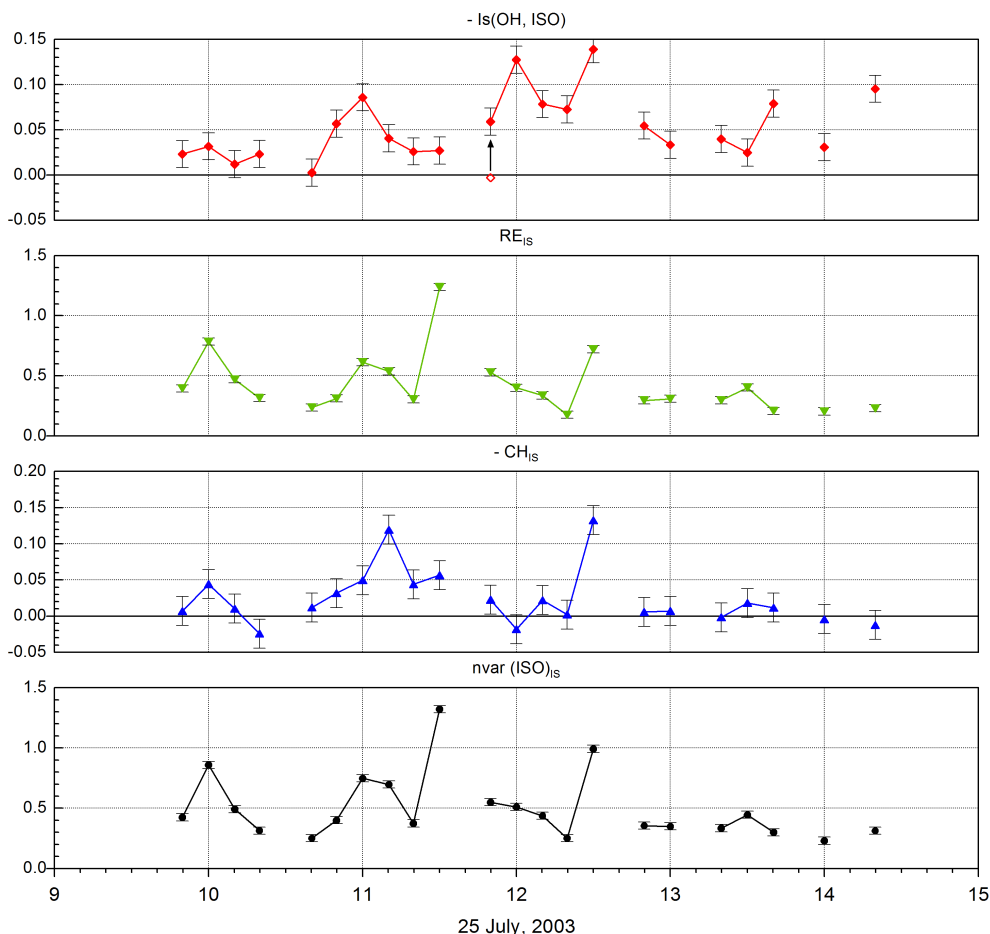
Figure 16. The four terms of Eq. (16) solved for RE_{is} as a function of time.

5.3.4 Sources of isoprene and OH and mixing

As mentioned in Sects. 4 and 5.3.2, one point around $I_S \simeq 0$ with $\sigma_i = 0.67$ (Figs. 4, 10, 11) and $R_{ij} = 2.78 \times 10^{-4} \, \text{ppb}^2 \, \text{s}^{-1}$ (Fig. 14) does not follow the general behaviour – namely that $-I_S$ increases with increasing σ_i and R_{ij}. The reason for this can be found if the spectral distribution of the covariance $\overline{c_i' c_j'}$, the ogive (Oncley, 1989; Beier and Weber, 1992), is considered (Fig. 17) for this 10 min time interval at 11:50 CET and compared – for example – to the time interval at 12:30 CET with the maximum value of $I_S = -0.14$. At 11:50 CET the influences of changing OH production rate by photolysis as well as isoprene emission cause a positive correlation between OH and isoprene in the low-frequency part of the time window of 10 min between 1.6×10^{-3} Hz and 0.2 Hz. The isoprene source strength E (e.g. Guenther et al., 1995, 2006) is significantly influenced by solar radiation and leaf surface (volume) temperature on timescales longer than about 30–60 s. The measurements of surface radiative temperature at main tower also show changes up to 4 K for the same timescales. Ciccioli et al. (1997) described the oscillation of leaf surface tem-

perature – caused by strongly variable solar radiation flux as also found on day 206 for ECHO 2003 (Dlugi et al., 2010) – and its influence on the variability of E and therefore also c_i. Also the influence of variation of $J(\text{O}^1\text{D})$ photolysis frequency can be directly found for time intervals longer than about 1 min (Dlugi et al., 2010). Both processes are related to each other by fluctuations of radiation quantities and are partly correlated. Therefore the covariance between OH and isoprene for time periods longer than about 60 s appears as a positive contribution to the ogive in the lower part of Fig. 17. In addition, for higher frequencies, mixing of both compounds is not complete as observed also for other time periods, e.g. at 12:30 CET (Figs. 16, 17). If integrated over the whole spectrum to calculate the covariance, the remaining negative contribution to I_S above 1.5×10^{-2} Hz from inhomogeneous mixing is compensated by the other part, which leads to $I_S \approx 0$.

If only the process of inhomogeneous mixing is considered, this type of ogive is given in the upper part of Fig. 17 for the maximum case but being in principle valid for all other data points except at 11:50 CET. The change of the ogive for inhomogeneous mixing is most significant below about
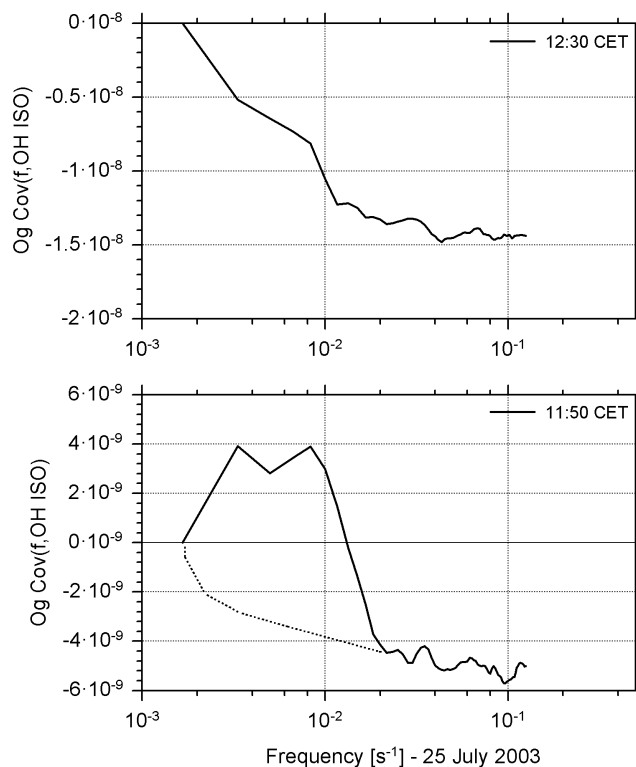
Figure 17. The spectral presentation of the ogives of the covariance of OH and isoprene for the maximum of I_S at 12:30 CET, and the minimum of I_S at 11:50 CET when both parts compensate each other and apparently result in $I_S \simeq 0$ (see Sect. 5.3.4). The broken line for the results at 11:50 CET shows a possible behaviour of the ogive if only inhomogeneous mixing occurs.

5×10^{-2} Hz suggesting also that the detection limit of both measuring devices (PTR-MS, LIF), causing a loss of high-frequency contributions as discussed by Dlugi et al. (2010), has no significant influence on these results. If one considers only the contribution from the negative part of the ogive at 11:50 CET, the corresponding data point moves to $I_S \simeq -0.06$ (see Fig. 4) for $R_{ij} = 2.78 \times 10^{-4}$ ppb^2 s^{-1} in Fig. 14 and for $\sigma_{ISO} = 0.67$ in Fig. 10.

If the negative part of the ogive is extrapolated to the lowest frequency, I_S becomes larger within the range $-0.095 \leq I_S < -0.13$ depending on the spectral dependence below 1.5×10^{-2} Hz as illustrated in Fig. 17. As this spectral behaviour needs some assumptions, only the value $I_S \simeq -0.06$ is given.

For other conditions the ogive (upper part of Fig. 17) shows that an estimate for the covariance, and I_S may be achieved even if the instruments have a time resolution of only about 0.06–0.2 Hz.

6 Potential influences of mixing processes

6.1 Eddy motion near canopy top

The relations between the covariance or I_S and different terms of their balance equations point towards the combined influences of chemical conditions as well as of turbulent transport and mixing processes near canopy top or even on a horizontally larger scale, e.g. by the influence of convection or small mesoscale circulation. On the smaller scale Katul et al. (1997) discussed the role of eddy motion near the forest–atmosphere interface. Also Patton et al. (2001) showed that coherent eddy motion and related mixing processes (with $r_{ij} \geq -0.8$) should influence the intensity of segregation I_S. In this paper such effects are related to terms like RE$_{is}$ and nvar(Iso)$_{is} = (\sigma_i/\overline{c_i})_{is}$. This is done without further specification of processes behind the nature of terms RES or RE$_{is}$ in Eqs. (15) and (16). For this purpose we calculated all terms of the Katul et al. (1997) version of third-order cumulant expansion method (CEM) to find out if the relative contribution of sweeps or ejections to the flux of isoprene can be related to the terms nvar(ISO)$_{is}$ or RE$_{is}$. A measure for this effect is the "stress function" ΔS_0 for the isoprene flux. This may be expressed in a simplified formulation derived from complete CEM (Katul et al., 1997; Cava et al., 2006) as

$$\Delta S_0 \approx \frac{1}{\sqrt{2\pi} \, 2R_{wc}} [M_{21} - M_{12}], \qquad (17)$$

with

$$M_{kl} = (\overline{c'^k w'^l})/(\sigma_c^k \, \sigma_w^l), \qquad (18)$$

and R_{wc} the correlation coefficient between the vertical velocity and isoprene mixing ratio in this case. M_{21} is a generalised correlation coefficient for the turbulent transport of isoprene variance and M_{12} the corresponding correlation coefficient for the turbulent flux of isoprene.

The "stress function" ΔS_0 neither from the complete CEM nor from the simplified parameterisation in Eq. (17) shows a significant correlation with I_S or terms of the balance in Eq. (16). But M_{21}, as the measure for turbulent transport of isoprene variance, shows some relation to RE$_{is}$ and nvar(Iso)$_{is}$ as presented in Fig. 18. Here a simple relation to M_{12} cannot be established. The smaller values of nvar(Iso)$_{is}$ correspond to small values of I_S (Fig. 10) and belong to smaller negative or positive M_{21} (Fig. 18). Therefore isoprene variance is vertically transported by turbulence in both directions but only upwards for larger values of nvar(Iso)$_{is}$. This agrees with the finding that upward-directed flux is related also to higher isoprene variance, and downdrafts are characterized by smaller values of σ_i or nvar(ISO)$_{is}$. A typical sweep ejection cycle, as often discussed in the literature (see discussion in Katul et al., 1997), cannot be simply established for chemical compounds in this data set. The
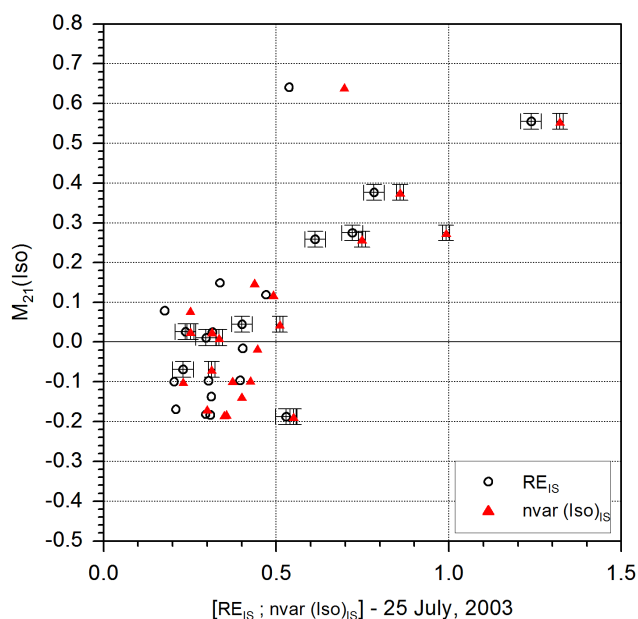
Figure 18. The correlation coefficient M_{21} (see Eq. 17) as a function of the two dominant terms nvar(Iso)$_{IS}$ and RE$_{IS}$ in the diagnostic equation to determine I_S (Eq. 16).

Figure 19. The intensity of segregation as a function of TKE.

behaviour for RE$_{is}$ is comparable as both terms are dominant and, therefore, are correlated to each other (Supplement Fig. S34).

6.2 Forced and free convective mixing

During the measuring period of 25 July 2003 (day 206) of ECHO 2003, the stratification varied between slightly stable to unstable conditions with a change from mechanically induced turbulence to nearly free convective conditions. This allows the comparison of the results from this field study to model results.

Recently Ouwersloot et al. (2011) showed that in a region with an inhomogeneous distribution of surface sensible heat fluxes H and, therefore, surface buoyancy flux H_v and isoprene emission fluxes, the segregation intensity for the reaction between isoprene and OH can increase with increasing differences ΔH_v between a cooler forest and a warmer savanna-type area. This situation is qualitatively comparable to the Jülich site as the deciduous forest is surrounded by urbanised area with buildings of the research centre and agricultural areas being dryer and, therefore, warmer than the forest canopy. Their results also point towards an increase in the turbulent kinetic energy (TKE) and also buoyant production BP – a term in the TKE balance – with increasing ΔH_v and even H_v itself. In their Fig. 13 they show a case with $I_S \approx -0.195$ for $\Delta H_v = 0$ and obviously a mean surface kinematic heat flux of $H = 0.15\,\mathrm{K\,m\,s^{-1}}$. But for their case with $\Delta H_v = 0$ still differences in isoprene emission fluxes (0.7 ppb m s^{-1}) are computed. Therefore homogeneous heat
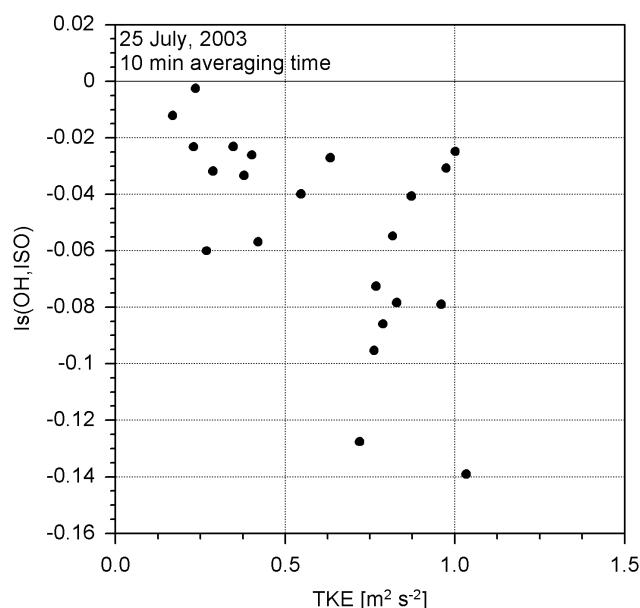
flux conditions are not identical to the homogeneous isoprene flux distribution in this model calculation. For this purpose one has to choose the case HOM ($I_S \approx -0.07$) for further comparison.

Their finding suggests that one should observe I_S increasing with TKE and with BP or H respectively H_v itself. These relations between I_S and TKE respectively BP from the ECHO measuring period (25 July 2003, 09:00–15:00 CET) are presented in Figs. 19 and 20. Indeed, the largest values for I_S are found for the largest values of TKE and BP, but – as discussed before (Sect. 5.3.2) – are for smaller values significantly modified by the influence of the chemical state of the reactant mixture. Therefore two data points with TKE $> 0.85\,\mathrm{m^2\,s^{-2}}$ have $I_S < -0.03$ because they are for the morning hours with larger mixing ratios of NO$_x$ which are conditions with lower mean percentage of OH reactivity related to isoprene as given in Fig. 4 and Tables 1 and 2. These results also belong to the data points in the blue circle in Fig. 4 between I_S and mean OH mixing ratio. Two other data points with $I_S = -0.06$ and $I_S = -0.057$ are for the lowest NO$_x$ mixing ratio and for TKE $< 0.5\,\mathrm{m^2\,s^{-2}}$, reflecting the possible variability by influences of chemistry and turbulent transport and mixing. Note that for these two points the friction velocity u_* is significantly lower than the convective scale velocity w_*. This hints towards a significant contribution of convection to vertical transport for both cases as can be seen for the relation between I_S and H respectively BP in Fig. 20. If these aspects are considered, I_S increases on average with increasing TKE in the range where chemical isoprene removal is influenced by concurrent reactants (e.g. $f < 0.9$, Sect. 2.3) up to about $I_S \simeq -0.04$. Larger values of
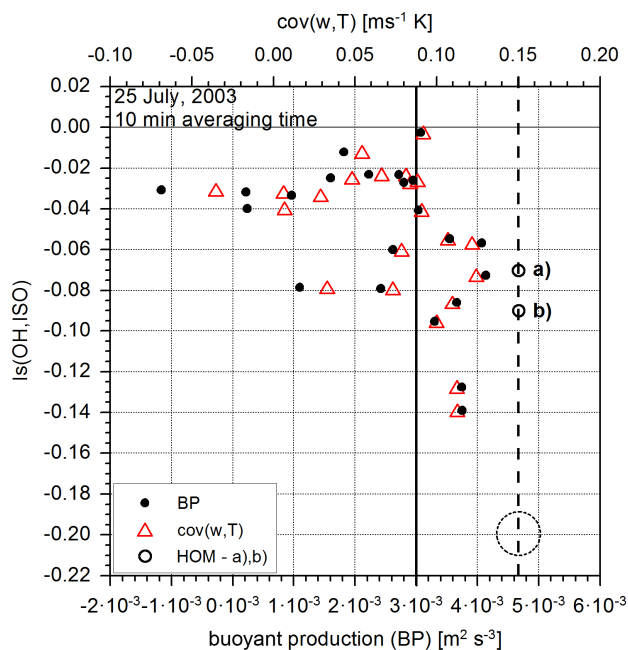
Figure 20. The intensity of segregation as a function of buoyant production (BP) and sensible heat flux H. The dotted circle and the data points labelled **(a)** and **(b)** indicates the range of results presented by Ouwersloot et al. (2011) and are explained in Sect. 6.2.

I_S are in the range with $f \geq 0.75$ where I_S becomes nearly independent of TKE.

As for TKE comparable findings are obtained for I_S as a function of BP (Fig. 20). The data points for low NO_x mixing ratios – as also found for the TKE–I_S–relation – are mainly in a range $BP > 3 \times 10^{-3}\,m^2\,s^{-2}$ and $|I_S| > 0.04$.

The behaviour of $-I_S$ as a function of BP shows an increase of $-I_S$ for $BP > 3.0 \times 10^{-3}\,m^2\,s^{-3}$, if two data points with $I_S = -0.078$ and $BP = 1.1 \times 10^{-3}\,m^2\,s^{-3}$ and $I_S = -0.079$ and $BP = 2.4 \times 10^{-3}\,m^2\,s^{-3}$ are neglected for this consideration. This range for BP is equivalent to a sensible heat flux $H > 0.08\,K\,m\,s^{-1}$, defining the conditions for the onset of convection at canopy top ($z_R/L_* > -1.0$) for which $I_S > -0.04$ is valid. If H_v is calculated instead of H, $H_v \simeq 1.08 \times H$ for $H > 0.06\,K\,m\,s^{-1}$ for this data set. An extrapolation of the data to $H_v = 0.15\,K\,m\,s^{-1}$ yields $I_S \gtrsim -0.2$, and a qualitative agreement with the model calculations by Ouwersloot et al. (2011). The footprint analysis (Figs. S19–S21 in the Supplement) reveals that the maxima in the amount of $-I_S$ agree also with the advection of isoprene from nearby emission from oaks in the south to southwest wind sector.

For nearly homogeneous conditions two data points (a) and (b) can be taken from their results for conditions HOM where homogeneous emissions of isoprene are modelled with $H_v = 0.15\,K\,m\,s^{-1}$. Therefore, depending on the spatial distribution of fluxes of isoprene and heat, I_S may differ up to a factor of about 3.

Also the dependence of the correlation coefficient r_{ij} as a function of the mean reaction rate $k_{ij} \times \overline{ISO} \times \overline{OH}$ given in Fig. 7 can be compared to results by Ouwersloot et al. (2011). They reported that the correlation coefficient increases with increasing reaction rate. The ECHO 2003 data have a maximum of $k_{ij} \times \overline{ISO} \times \overline{OH} \approx 6.9 \times 10^{-4}\,ppb\,s^{-1}$ (Fig. 7), which is somewhat larger than given by Ouwersloot et al. (2011) in their Fig. 4. Their corresponding correlation coefficient given near the surface is significantly larger but for mean mixing ratios of $\overline{OH}$ about one-third of the ECHO 2003 data and about a 3-fold mixing ratio of isoprene. Note that the chemical regime is different with $NO_x < 1$ ppb for the model study and $NO_x \geq 2$–3 ppb for the ECHO field study. The results of Fig. 13 of Ouwersloot et al. (2011) show that I_S is a function of ΔH_v. A comparable spatial variability of H_v may be possible for ECHO 2003 because of the inhomogeneous distribution of forest areas around the main tower and the influence of buildings, roads and grassland at the Jülich Research Centre (e.g. Aubrun et al., 2005). This type of landscape suggests that the result from Sect. 5.2 that the horizontal derivations of term A_{2k} should significantly modify RES and RE_{is} in Eqs. (15)–(16) to achieve $S \simeq 0$ may be caused by this influence of inhomogeneous distributed sources of heat and isoprene, which are also modified by cloud-driven convection and an inhomogeneous distribution of radiation fluxes.

6.3 Damköhler number dependence

Some authors related the effective rates of second-order chemical reactions and also the segregation intensity I_S to specific Damköhler numbers Da_c of specific compounds c_i. For the situation during ECHO 2003, the only available study at least for a qualitative comparison of the dependence of I_S on Da_c is from Patton et al. (2001). Their results from a LES modelling study are for a forest with a comparable leaf area index and canopy height $h_c = 20\,m$ (ECHO: $h_c = 30\,m$). For the model study Da_c for isoprene is defined by $Da_c = \frac{\tau_t}{\tau_c} = \frac{h_c}{u_*} \times k_{ij} \times \overline{OH}$. While $u_* = 0.28\,m\,s^{-1}$ in this model study the friction velocity from the field experiment during the considered time period is in the range $0.12 \leq u_* \leq 0.71\,m\,s^{-1}$ with a mean value $\overline{u_*} = 0.39\,m\,s^{-1}$ (see Fig. 3 in Dlugi et al., 2010). Therefore, in the field τ_t varied by a factor of about 6 by the influence of u_*, and Da_c is not only modified by $\overline{OH}$ like in the model study by Patton et al. (2001). A comparison with this model study can only be performed if OH_{mod} is applied in the definition of Da_c because this quantity is comparable to the NO_x-free system as used in their model. OH and OH_{mod} are comparable with OH mixing ratios in the model studies, e.g. about 1.2×10^{-4} ppb for the volume average $\overline{OH_v}$ for $Da_c = 0.02$ compared to the data presented in Fig. 1. For the model study Da_c increases linearly with $\overline{OH_v}$, and, therefore, for $Da_c = 0.1$ a significantly higher mixing ratio of $\overline{OH_v} = 6 \times 10^{-4}$ ppb is calculated than obtained in the field. Not only the chemical system is different. The model describes free convective conditions

with the kinematic sensible flux of $0.35\,\mathrm{K\,m\,s^{-1}}$, also significantly larger than measured in the field (Fig. 20).

This value is estimated from their sensible heat flux $H = 0.43\,\mathrm{K\,m\,s^{-1}}$ (page 25 of Patton et al., 2001). If we instead take the reported stability parameter $h_c/L_* = -0.4$, their sensible heat flux is of the order of $0.1\,\mathrm{K\,m\,s^{-1}}$ and, therefore, comparable to our data from the field.

The calculated Damköhler numbers Da_c for the chemical removal of isoprene by OH during ECHO 2003 are given in Fig. 21. A chemical plausible result is obtained only on the right part for the dependence of I_S on $Da_{c,\mathrm{mod}}$ with $\overline{\mathrm{OH}}$ substituted by $\overline{\mathrm{OH}}_{\mathrm{mod}}$. Here I_S increases on average with increasing mixing ratio $\overline{\mathrm{OH}}_{\mathrm{mod}}$ for the effective chemical sink for isoprene with the exception of two data points. The relation $I_S \sim f(Da_c)$ seems to be different for $I_S < -0.04$ and $I_S > -0.04$. Such a behaviour is also suggested by the results given in Fig. 4 of Patton et al. (2001). For a linear interpolation through zero, on average, the ECHO data yield $I_S \approx -2.7 \times Da_{c,\mathrm{mod}}$ for an atmosphere which is influenced by shear-driven and convective-driven turbulence roughly separated by the line through $H = 0.085\,\mathrm{K\,m\,s^{-1}}$ in Fig. 20. Patton et al. (2001) obtained $I_S \simeq -0.175$ for $Da_c = 0.17$ while a comparable linear extrapolation through zero from the ECHO data set yields a similar value of $I_S \approx -0.175$ for $Da_c \simeq 0.065$. The effective turbulent exchange process during free convective conditions is rather different compared to shear-driven turbulence (Stull, 1988). Also the application of the applied definition of $Da_c \sim u_*^{-1}$ can only be an estimate for convective conditions. Therefore, although the conditions in the field significantly differ from those of the model study (Patton et al., 2001), the experimental and model results quantitatively agree with respect to the increase of I_S with increasing Da_c. Formally OH is produced and destroyed only on a local-scale with $\tau_c < 0.2\,\mathrm{s}$. If we estimate a mean transport timescale τ_t for that volume by the wind velocity components, we obtain $\tau_t > 1\text{--}3\,\mathrm{s}$. Therefore, $\tau_c \ll \tau_t$, and with $k_{ij} = 2.3\,\mathrm{ppb^{-1}\,s^{-1}}$ and $c_i \approx 1\,\mathrm{ppb}$ one obtains a large Damköhler number for OH given by $\tau_t/\tau_c = D_{\mathrm{iso}} > 20$ as required for a fast reacting compound.

7   Summary

The terms of the balances of mixing ratio of isoprene, the covariance $\overline{c_i\, c_j}$ and the segregation intensity I_S are compared to each other. For the mixing ratio the storage term is compensated by a residuum which is mainly composed by the divergence of the turbulent flux as well as by (unknown) contributions from advection because both terms of the chemical sink are smaller. Within this chemical term the covariance between isoprene and OH is less than 15 % of the product of the means of the mixing ratios. The quotient of both terms, the intensity of segregation I_S, increases with mean OH mixing (c_i) ratio as well as standard deviation of isoprene σ_i and normalised variance. The further data analy-

sis shows that both findings from the ECHO field study are at least partly and qualitatively comparable to model results by Patton et al. (2001). Therefore, for increasing σ_i, I_S increases with the restriction that other chemical compounds reacting with OH at comparable reaction rates reduce the degree of inhomogeneous mixing for the isoprene–OH reaction. The estimation of the contribution of isoprene to $\overline{\mathrm{OH}}$ removal – expressed as $\mathrm{OH}_{\mathrm{mod}}$ – is estimated by a relationship considering chemical sources and sinks of OH. A factor f is calculated and shows that the correlation between I_S and the modelled $\overline{\mathrm{OH}}_{\mathrm{mod}}$ is significantly enhanced compared to measured $\overline{\mathrm{OH}}_{\mathrm{meas}} = \mathrm{OH}$.

Based on these relations used in models, the same concept is independently used here to analyse the measured data. The concept applied the balance equation for the covariance between isoprene and OH as a rule and allows us to further evaluate the data. In this way, the contributions of all processes, which are represented by different terms in this equation, to the covariance – and therefore to the transport terms – can be estimated for the field data from ECHO 2003. The storage term is found to be small compared to other terms of the balance. This allows us to formulate a new diagnostic version of the balance equation also to relate turbulent and advective transport and mixing terms (RES and RE_{is}) and influences of chemical reactions (R_{ij}) to the intensity of segregation I_S. The following analysis shows that the reaction rate R_{ij} is largely dominated by the variance of isoprene $\mathrm{var(Iso)}_{is}$ times the quotient $(\overline{\mathrm{OH}} / \overline{\mathrm{ISO}}) \times k_{ij}$, which supports the findings discussed above. This is the reason why I_S and R_{ij} show a better relation to the normalised variance than to the variance, as earlier suggested by Patton et al. (2001) and Davis (1992) (more details can be found in the Supplement). This is probability caused by the fact that isoprene is not the only chemical sink for OH in the field study in contrast to the model studies or measurements in really remote areas.

The results prove that the chemical term and the transport and mixing term are of nearly equal influence on the covariance and, therefore, I_S. Some data points show deviations from simple relations. These are caused by dynamics different from the general picture that isoprene is emitted at the surface, mixed upward and reacted with locally produced OH as well as by possible short time deviation of factor f from its mean $\overline{f}$.

The detailed spectral analysis of the ogive of $\overline{c_i'\, c_j'}$ shows that a case with an apparent value $I_S \simeq 0$ is obtained at $11{:}50\,\mathrm{CET}$ by a counteracting influence of the time-dependent positively correlated change of OH production and isoprene emission for lower frequencies together with inhomogeneous mixing for higher frequencies. If only the process of inhomogeneous mixing is considered, a value $I_S \simeq -0.06$ is estimated, which corrects results earlier published by Dlugi et al. (2010). In general, for this field study, I_S can be related to the dominant term in the chemical reaction term – the normalised variance of isoprene – and to the
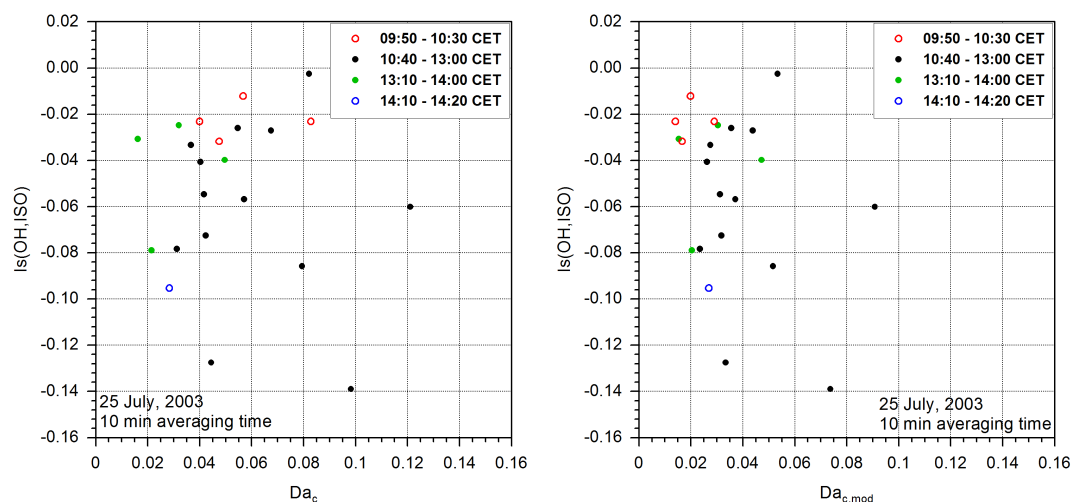
Figure 21. I_S as a function of Damköhler numbers Da_c (left) and $Da_{c\mathrm{mod}}$ (right) for the time periods from Tables 1 and 2 with OH substituted by modelled OH_{mod}.

action of the residual terms RES or RE_{is}. If their difference increases, $-I_S$ increases as well. This points towards a decreasing influence of concurrent chemical reaction cycles on I_S (Table 2) and is an indication of a smaller relative contribution of advection compared to convective transport within terms RES and RE_{is} for larger values of $-I_S$ for the conditions of this field study.

On the one hand for a negligible influence of RES respectively RE_{is}, one may simply estimate a maximum value of I_S by the variance term $\mathrm{nvar(ISO)}_{is}$ itself with consideration of the reactivity of the chemical system (Table 1, 2). On the other hand, I_S can approach small values, although reaction conditions suggest $I_S > -0.04$, only by the influence of RE_{is}.

Within this framework the processes influencing the terms $\mathrm{nvar(ISO)}_{is}$ and RE_{is} remain undefined. Therefore a different additional analysis to find out at least physical parameter controlling exchange and mixing and revealing some relation to I_S is performed.

An indicator ΔS_0 for the amount of appearance and influence of coherent eddies on the flux of isoprene shows no clear relation to I_S or other terms of its balance. But a relation between the correlation coefficient for the turbulent transport of isoprene variance M_{21} is found with the normalised variance of isoprene $\mathrm{nvar(ISO)}_{is}$ itself as well as the residuum RE_{is}. This hints towards the influence of turbulent transport of isoprene variance on the residual term RE_{is}.

In addition, the absolute value of I_S shows a tendency to increase with increasing turbulent kinetic energy TKE and buoyant production BP if concurrent chemical reactions are of less influence.

These results qualitatively agree with findings by Ouwersloot et al. (2011) on an increase of $-I_S$ with increasing influence of turbulent mixing and convection. This effect can only be evaluated from data for conditions when isoprene is the main sink for OH. Otherwise, if the reaction rates of concurrent chemical reactions are dominant, the segregation intensity for the reaction isoprene + OH is found to be equal to or below $I_S = -0.04$.

If the Damköhler number Da_c is applied to describe the reaction by the influence of shear-driven turbulence, an increase of $|I_S|$ with increasing $Da_{c,\mathrm{mod}}$ is found. This finding only qualitatively agrees with model results by Patton et al. (2001) because mixing conditions and chemical conditions from the field are different.

In addition, if measurements were performed with a smaller time resolution of about 0.06–0.2 Hz our analysis of the ogives (Sect. 5.3.4) shows that estimates of I_S can still be achieved to compare to other results from the field and model studies.

Appendix A

Table A1. List of symbols.

index l, k	representing any chemical compound, i.e. Eqs. (1)–(4)
index i	representing isoprene (ISO), i.e. Eq. (2)
index j	representing OH radical (OH), i.e. Eqs. (1) and (3)–(4)
index is	term which belongs to diagnostic equation for I_S
c_k	mixing ratio of compound k
$\bar{c}_k$	mean mixing ratio of compound k
$c'_k = c_k - \bar{c}_k$	deviation from mean mixing ratio
k_{lk}	reaction rate constant for reaction between compounds l and k
k_{ij}	reaction rate constant for reaction between isoprene and OH
$\overline{c'_i c'_j}$	covariance between reactants by turbulent fluctuations of both compounds i and j
$\overline{w' c'_k}$	turbulent vertical flux for chemical compound k
r_{ij}	correlation coefficient between turbulent fluctuations of compounds i and j
I_S	segregation intensity as defined in Eq. (7)
σ_k	standard deviation of compound k
$\sigma_i = \sigma(\text{ISO})$	standard deviation of isoprene
$\sigma_j = \sigma(\text{OH})$	standard deviation of OH
$\sigma_k / \bar{c}_k$	normalised standard deviation of compound k
$\text{var(ISO)} = \sigma_i^2 = \overline{c_i'^2}$	variance of turbulent isoprene fluctuations
$\text{var(OH)} = \sigma_j^2 = \overline{c_j'^2}$	variance of turbulent OH fluctuations
$\text{nvar(ISO)} = \sigma_i^2 / \bar{c}_i^2$	normalised variance of turbulent isoprene fluctuations
$\text{nvar(OH)} = \sigma_j^2 / \bar{c}_j^2$	normalised variance of turbulent OH fluctuations
ΔS_0	"stress function" in Eq. (17)
M_{21}	generalized correlation coefficient for turbulent transport of isoprene variance (Eq. 17)
M_{12}	generalized correlation coefficient for turbulent transport of the turbulent flux of isoprene
R_{wc}	correlation coefficient between the turbulent fluctuations of vertical velocity and isoprene mixing ratio
TKE	turbulent kinetic energy [m^2 s^{-2}]
BP	buoyant production [m^2 s^{-3}]
$Da_c = \tau_t / \tau_c$	quotient between characteristic timescales of turbulent or convective (Introduction, Sect. 6.3)
(Damköhler number)	mixing τ_t and specific chemical reaction time τ_c
u_*	friction velocity [m s^{-1}]
w_*	convective velocity scale [m s^{-1}]
RES	residual term in Eqs. (13) and (15) which describes the influence of advective and turbulent interaction of the flow and the reactant
RE_{is}	normalised residual RES in Eq. (16)
R_{ij}	chemical reaction term in Eq. (9)

References

Ammann, C., Spirig, C., Neftel, A., M., S., Komenda, M., and Schaub, A.: Application of PTR-MS for measurements of biogenic VOC in a deciduous forest, Int. J. Mass Spectrom., 239, 87–101, 2004.

Aubrun, S., Koppmann, R., Leitl, B., Möllmann-Coers, M., and Schaub, A.: Physical modelling of a complex forest area in a wind tunnel – comparison with field data, Agr. Forest. Meteorol., 129, 121–135, 2005.

Beier, N. and Weber, M.: Turbulente Austauschprozesse in der Grenzschicht, Tech. rep., Meteorologisches Institut, Universität München, Germany, 1992.

Bencula, K. and Seinfeld, J.: On frequency distributions of air pollutant concentrations, Atmos. Environ., 10, 941–950, 1976.

Bohn, B.: Solar spectral actinic flux and photolysis frequency measurements in a deciduous forest, J. Geophys. Res., 111, D15303, doi:10.1029/2005JD006902, 2006.

Bohn, B., Kraus, A., Müller, M., and Hofzumahaus, A.: Measurment of atmospheric $O_3 \rightarrow O^1D$ photolysis frequencies using filterradiometry, J. Geophys. Res., 109, D10S90, doi:10.1029/2003JD004319, 2004.

Bohn, B., Koppmann, R., and Rohrer, F.: Seasonal variations and profile measurements of photolysis frequencies $j(O^1D)$ and $j(NO_2)$ at the ECHO forest field site, J. Geophys. Res., 111, D12303, doi:10.1029/2005JD006856, 2006.

Butler, T. M., Taraborrelli, D., Brühl, C., Fischer, H., Harder, H., Martinez, M., Williams, J., Lawrence, M. G., and Lelieveld, J.: Improved simulation of isoprene oxidation chemistry with the ECHAM5/MESSy chemistry-climate model: lessons from the GABRIEL airborne field campaign, Atmos. Chem. Phys., 8, 4529–4546, doi:10.5194/acp-8-4529-2008, 2008.

Cava, D., Katul, G. G., Scrimieri, A., Poggi, D., Cescatti, A., and Giostra, U.: Buoyancy and the sensible heat flux budget within dense canopies, Bound.-Lay. Meteorol., 118, 217–240, 2006.

Ciccioli, P., Fabozzi, C., Brancaleoni, E., Cecinato, A., Frattoni, M., Loreto, F., Kesselmeier, J., Schäfer, L., Bode, K., Torres, L., and Fugit, J.-L.: Use of the isoprene algorithm for predicting the monoterpene emission from the Mediterranean holm oak Quercus ilex L.: Performance and limits of this approach, J. Geophys. Res., 102, 23319–23328, 1997.

Damköhler, G.: Einfluß von Diffussion, Strömung und Wärmetransport auf die Ausbeute bei chemisch-technischen Reaktionen, VDI, Leverkusen, 1957.

Danckwerts, P.: The definition and measurement of some characteristics of mixtures, Appl. Sci. Res., 3, 279–296, 1952.

Davis, K.: Surface fluxes of trace gases derived from convective profiles, Ph.D. thesis, Univ. of Colorado, Boulder, 1992.

Dlugi, R., Berger, M., Zelger, M., Hofzumahaus, A., Siese, M., Holland, F., Wisthaler, A., Grabmer, W., Hansel, A., Koppmann, R., Kramm, G., Möllmann-Coers, M., and Knaps, A.: Turbulent exchange and segregation of HOx radicals and volatile organic compounds above a deciduous forest, Atmos. Chem. Phys., 10, 6215–6235, doi:10.5194/acp-10-6215-2010, 2010.

Donaldson, C. D.: Construction of a Dynamic Model of the Production of Atmospheric Turbulence and the Dispersal of Atmospheric Pollutants, in: Workshop on Micrometeorology, edited by: Haugen, D., 313–393, American Meteorological Society, Boston, 1973.

Donaldson, C. D.: On the modelling of the scalar correlation necessary to construct a second order closure description of turbulent reacting flows, in: A review in turbulent mixing in non reactive and reactive flows, edited by: Murthy, S., Plenum Press, New York, 1975.

Donaldson, C. D. and Hilst, G.: Effect of inhomogeneous mixing on atmospheric photochemical reactions, Environ. Sci. Technol., 6, 812–816, 1972.

Ebel, A., Memmesheimer, M., and Jakobs, H. J.: Chemical perturbations in the planetary boundary layer and their relevance for chemistry transport modelling, Bound.-Lay. Meteorol., 125, 256–278, 2007.

Finlayson-Pitts, B. J. and Pitts Jr., J. N.: Atmospheric Chemistry: Fundamentals and Experimental Techniques, J. Wiley & Sons, New York, 1986.

Guenther, A., Hewitt, C. N., Erickson, D., Fall, R., Geron, C., Graedel, T., Harley, P., Klinger, L., Lerdau, M., McKay, W. A., Pierce, T., Scholes, B., Steinbrecher, R., Tallamraju, R., Taylor, J., and Zimmerman, P.: A global model of natural volatile organic compound emissions, J. Geophys. Res., 100, 8873–8892, 1995.

Guenther, A., Karl, T., Harley, P., Wiedinmyer, C., Palmer, P. I., and Geron, C.: Estimates of global terrestrial isoprene emissions using MEGAN (Model of Emissions of Gases and Aerosols from Nature), Atmos. Chem. Phys., 6, 3181–3210, doi:10.5194/acp-6-3181-2006, 2006.

Holland, F., Hessling, M., and Hofzumahaus, A.: Insitu measurement of tropospheric OH radicals by laser-induced fluorescence – a description of the KFA instrument, J. Atmos. Sci., 52, 3393–3401, 1995.

Holland, F., Hofzumahaus, A., Schäfer, J., Kraus, A., and Pätz, H.-W.: Measurements of OH and HO$_2$ radical concentrations and photolysis frequencies during BERLIOZ, J. Geophys. Res., 108, 8246, doi:10.1029/2001JD001393, 2003.

Hollinger, D. Y. and Richardson, A. D.: Uncertainty in eddy covariance measurements and its application to physiological models, Tree Physiol., 25, 873–885, 2005.

Katul, G. G., Msieh, C.-I., Kuhn, G., Ellsworth, D., and Nie, D.: Turbulent eddy motion at the forest-atmosphere interface, J. Geophys. Res., 102, 13407–13421, 1997.

Kleffmann, J., Gavriloaiei, T., Hofzumahaus, A., Holland, F., Koppmann, R., Rupp, L., Schlosser, E., Siese, M., and Wahner, A.: Daytime formation of nitrous acid: A major source of OH radicals in a forest, Geophys. Res. Lett., 32, L05818, doi:10.1029/2005GL022524, 2005.

Kramm, G. and Meixner, F. X.: On the dispersion of trace species in the atmospheric boundary layer:A re-formulation of the governing equations for the turbulent flow of the compressible atmosphere, Tellus A, 52, 500–522, 2000.

Kramm, G., Dlugi, R., Dollard, G. J., Foken, T., Mölders, N., Müller, H., Seiler, W., and Sievering, H.: On the dry deposition of ozone and reactive nitrogen species, Atmos. Environ., 29, 3209–3231, 1995.

Krol, M. C., Molemaker, M.-J., and Vilà Guerau de Arellano, J.: Effects of turbulence and heterogeneous emission on photochemically active species in the convective boundary layer, J. Geophys. Res., 105, 6871–6884, doi:10.1029/1999JD900958, 2000.

Lamb, R. and Seinfeld, J.: Modeling for urban air pollution – general theory, Environ. Sci. Technol., 7, 253–261, 1973.

Lamb, R. and Shu, W.: A Model of second order chemical reactions in turbulent fluid – part I: Formulation and Validation, Atmos. Environ., 12, 1685–1694, 1978.

Lenschow, D. H.: Reactive trace species in the boundary layer from a micrometeorological perspective, J. Meteorol. Soc. Jpn., 60, 472–480, 1982.

McRae, G., Goodin, W., and Seinfeld, J.: Mathematical modelling of photochemical air pollution, EQL-Report No.18, Tech. rep., California Inst.of Technology, Pasadena, 1982.

O'Brien, E. E.: Turbulent mixing of two rapidly reacting chemical species, Phys. Fluids, 14, 1326–1331, 1971.

Oncley, S. P.: Flux Parameterization Techniques in the Atmospheric Surface Layer, Ph.D. thesis, University of California, Irvine, CA, USA, 1989.

Ouwersloot, H. G., Vilà-Guerau de Arellano, J., van Heerwaarden, C. C., Ganzeveld, L. N., Krol, M. C., and Lelieveld, J.: On the segregation of chemical species in a clear boundary layer over heterogeneous land surfaces, Atmos. Chem. Phys., 11, 10681–10704, doi:10.5194/acp-11-10681-2011, 2011.

Patton, E., Davis, K., Barth, M., and Sullivan, P. P.: Decaying scalars emitted by a forest canopy: A numerical study, Bound-Lay. Meteorol., 100, 91–129, 2001.

Press, W. H., Flannery, B. P., Teukolsky, S. A., and Vetterling, W. T.: Numerical Recipes, Cambridge University Press, Cambridge, UK, 1991.

Pugh, T. A. M., MacKenzie, A. R., Langford, B., Nemitz, E., Misztal, P. K., and Hewitt, C. N.: The influence of small-scale variations in isoprene concentrations on atmospheric chemistry over a tropical rainforest, Atmos. Chem. Phys., 11, 4121–4134, doi:10.5194/acp-11-4121-2011, 2011.

Sachs, L. and Hedderich, J.: Angewandte Statistik, Springer, Berlin, Heidelberg, New York, 2006.

Schaub, A.: Untersuchung von Isopren und dessen Oxidationsprodukten in und oberhalb eines Mischwaldes, Ph.D. thesis, Mathematisch-Naturwissenschaftliche Fakultät, Universität Köln, Germany, 2007.

Schumann, U.: Large-eddy simulation of turbulent diffusion with chemical reactions in the convective boundary layer, Atmos. Environ., 23, 1713–1729, 1989.

Seinfeld, J. H. and Pandis, S. N.: Atmospheric Chemistry and Physics, John Wiley & Sons, New York/Chichester/Weilheim/Brisbane/Singapore/Toronto, 1997.

Shu, W.: Turbulent chemical reactions: Application to atmospheric chemistry, Ph.D. thesis, Dept. Chem. Eng., Caltec, Pasadena, 1976.

Sorbjan, Z.: Structure of the atmospheric boundary layer, Prentice Hall, N. J., USA, 1989.

Spirig, C., Neftel, A., Ammann, C., Dommen, J., Grabmer, W., Thielmann, A., Schaub, A., Beauchamp, J., Wisthaler, A., and Hansel, A.: Eddy covariance flux measurements of biogenic VOCs during ECHO 2003 using proton transfer reaction mass spectrometry, Atmos. Chem. Phys., 5, 465–481, doi:10.5194/acp-5-465-2005, 2005.

Stockwell, W. R.: Effects of turbulence on gas-phase atmospheric chemistry: Calculation of the relationship between time scale for diffusion and chemical reaction, Meteorol. Atmos. Phys., 57, 159–171, 1995.

Stull, R. B.: An Introduction to Boundary Layer Meteorology (Atmospheric Sciences Library), Springer, 1988.

Sun, J.: Tilt correction over complex terrain and their implication for CO_2-transport, Bound.-Lay. Meteorol., 124, 143–159, 2007.

Sykes, R. I., Parker, S. F., Henna, D. S., and Lewellen, W. S.: Turbulent Mixing with Chemical Reaction in the Planetary Boundary Layer, J. Appl. Meteorol., 33, 825–834, 1994.

van Stratum, B. J. H., Vilà-Guerau de Arellano, J., Ouwersloot, H. G., van den Dries, K., van Laar, T. W., Martinez, M., Lelieveld, J., Diesch, J.-M., Drewnick, F., Fischer, H., Hosaynali Beygi, Z., Harder, H., Regelin, E., Sinha, V., Adame, J. A., Sörgel, M., Sander, R., Bozem, H., Song, W., Williams, J., and Yassaa, N.: Case study of the diurnal variability of chemically active species with respect to boundary layer dynamics during DOMINO, Atmos. Chem. Phys., 12, 5329–5341, doi:10.5194/acp-12-5329-2012, 2012.

Verver, G., van Dop, H., and Holtslag, A.: Turbulent mixing of reactive gases in the convective boundary layer, Bound.-Lay. Meteorol., 85, 197–222, 1997.

Verver, G. H. L., van Dop, H., and Holtslag, A. A. M.: Turbulent mixing and the chemical breakdown of isoprene in the atmospheric boundary layer, J. Geophys. Res., 105, 3983–4002, 2000.

Vilà-Gureau de Arellano, J. and Duynkerke, P.: Influence of chemistry on flux gradient relationship for the NO-NO_2-O_3 System, Bound.-Lay. Meteorol., 61, 375–387, 1992.

Vilà-Guerau de Arellano, J. and Lelieveld, J.: Chemistry in the atmospheric boundary layer, in: Clear and Cloudy Boundary Layers, edited by: Holtslag, A. and Duynkerke, P., 267–286, Royal Netherlands Academy of Arts and Sciences, Amsterdam, the Netherlands, 1998.

Vilà-Guerau de Arellano, J., Duynkerke, P., and Builtjes, P.: The divergence of the turbulent diffusion flux in the surface layer due to chemical reactions: The NO-O_3-NO_2 system, Tellus, 43, 22–23, 1993.

Vilà-Guerau de Arellano, J., Duynkerke, P., and Zeller, K.: Atmospheric surface layer similarity theory applied to chemical reactive species, J. Geophys. Res., 100, 1397–1408, 1995.

Vinuesa, J.-F. and Vilà-Guerau de Arellano, J.: Introducing effective reaction rates to account for the inefficient mixing of the convective boundary layer, Atmos. Environ., 39, 445–461, 2005.

Wahrhaft, Z.: Passive scalars in turbulent flows, Annu. Rev. Fluid Mech., 32, 203–240, 2000.